

SIXTH INTERNATIONAL WORKSHOP on TROPICAL CYCLONES

Topic 1.2 : Tropical Cyclone Inner Core Dynamics

Rapporteur: Jeff D. Keper
Bureau of Meteorology Research Centre,
GPO Box 1289K
Melbourne, Australia

Email: J.Keper@bom.gov.au
Phone: +61+3+9669 4492
Fax: +61+3+9669 4660

Working Group: Michael Foley, Jeff Hawkins, Jim Kossin, David Nolan, Melinda Peng, Roger Smith, Yuqing Wang, Samuel Westrelin

1.2.1. Introduction

The inner core of a tropical cyclone contains the strongest winds, and is therefore of considerable practical importance. Apart from the direct impact, it is here that the bulk of the sea-air energy flux that sustains the storm occurs, that much of the ocean response in the form of storm surge, waves and currents are generated, and that the processes that lead to intensity change take place. The considerable forecast challenge of intensity change depends on both the hard to observe and assimilate inner core processes, as well as on environmental forcing. In contrast, track forecasting, with the exception of small-scale trochoidal oscillations, depends on larger-scale processes in the environment that are easier to discern.

The past few years have seen huge improvements in our ability to observe the inner core, both through in situ means, and by remote sensing. Examples include the GPS dropsonde, step frequency microwave radiometer, aircraft (now deployed by Taiwan and Canada as well as the USA), Doppler and conventional radar, passive microwave sensors, satellite sounders, rapid-scan satellite imagers, scatterometers, and portable towers and profilers, to name just a few.

Some substantial theoretical advances, coupled with the ability to learn from ever-higher resolution simulation, have complemented the observational increases.

These improvements have also led directly to operational advances, including an enhanced ability to monitor the eyewall replacement cycle, and the ability of operational NWP to predict intensity change and genesis, albeit to a limited degree.

This report will detail these advances, and is organised as follows. In section 1.2.2 we consider the boundary layer, which is important to understanding and ameliorating storm impact, to diagnosing storm intensity, to understanding the sea-air and land-air interactions that govern the energy supply to and dissipation of the storm, and to predicting the ocean response. Section 1.2.3 describes the symmetric and asymmetric structure of the eye and eyewall, including advances in our ability to monitor changes in this area. Section 1.2.4 considers the multiple types of spiral bands observed. Implications for forecasting are summarised in section 1.2.5, a summary of conclusions presented in section 1.2.6, and recommendations for research and operations made in section 1.2.7.

1.2.2. Boundary Layer

It is less than a decade since the first operational deployment of a GPS dropsonde (Hock and Franklin 1999) into a hurricane. This and other new observing technologies, coupled with theoretical advances, have resulted in an explosion in knowledge of the tropical cyclone boundary layer (TCBL), and the overturning of some long-established ideas and practices.

1.2.2.1 Mean structure

a) Observations

Observed wind profiles in tropical cyclones (TCs) frequently show a marked low level wind maximum. This maximum typically occurs around 300 to 800 m height near the eyewall, and 1 to 2 km at larger radius, and has been observed by dropsonde (e.g. Franklin et al., 2003), wind profiler (e.g. Knupp et al., 2000, 2005), and Doppler radar (e.g. Marks et al., 1999), although it has been the advent of the GPS dropsonde that has emphasised the frequent occurrence of this jet. The broad maximum is generally more-or-less obscured by smaller-scale fluctuations due presumably to turbulence, thus some form of averaging is needed to expose it clearly. For example, Fig 1.2.1 shows the observed mean normalised wind speed profile from the eyewall of seven hurricanes, in which this feature is clearly apparent. Below the jet, in the lowest 100 – 200 m, the wind speed increases nearly logarithmically with height, (Franklin et al., 2003; Powell et al., 2003), consistent with classical theory for a neutrally-stratified surface layer.

A substantial amount of between-storm variability is obvious in Fig 1.2.1. The strength of the normalised maximum varies from 1.12 to 1.3, and its height from 300 to 800 m, while the strength of the normalised surface wind speed is between 0.82 and 0.96. Franklin et al. (2003) speak of the differing “character” between individual storms; we will return to this matter later.

Along with variation between storms, there is substantial variation within each storm. The decrease in height of the low-level jet with decreasing radius becomes quite marked across the eyewall, and continues to the centre of the storm (Franklin et al., 2003; Kepert, 2002c, 2006a, b). Fig 1.2.2 shows the observed mean storm-relative wind profile in several annular regions in Hurricane Mitch (1998); it is clear that the depth of the frictional inflow layer and the jet height decrease towards the centre. Moreover, the azimuthal-wind maximum is generally near the top of, but within, the frictional inflow layer. Within the eye itself, both individual and mean soundings generally show little, if any, evidence of frictional retardation at the surface.

This radial variation in wind structure is accompanied by a variation in the surface wind factor (SWF); that is, the ratio of the near-surface wind speed to that at some higher level. Franklin et al. (2003) showed that the widely used value of 0.8 is appropriate for the outer vortex, but that this increased to 0.9 near the eyewall. They also found that the SWF varied with reference height, recommended higher values in the outer vortex near convection than in its absence, and noted higher values on the left of the storm track than on the right. These new values revised long-standing operational practice at the NHC, and were an important influence on the reanalysis of Hurricane Andrew’s landfall intensity to Saffir-Simpson category 5 (Landsea et al., 2004).

The SWF has been analysed in individual storms by Kepert (2002c, 2006a,b) and Schwendike (2004). The increase towards the storm centre is clearly marked, and some storms display higher values on the left of track than on the right. However other factors, including proximity to land in the case of Hurricane Mitch (1998), can also produce a significant asymmetry. Surface wind data from the airborne step-frequency microwave radiometer (SFMR) usually shows an increase in SWF towards the centre, and often a left-right asymmetry as well (Mark Powell, personal communication, 2006).

There is also a marked azimuthal variation in TCBL wind structure. Fig 1.2.3 shows the observed profiles in Hurricane Georges (1998). It is clear that a large part of the variability between profiles is due

to their position within the storm (Kepert, 2006a); this is especially striking as observations nearby in storm-relative space are not necessarily nearby in time. The height and strength of the low-level jet, and the depth and strength of the inflow layer, vary consistently around the storm. Analyses of Hurricanes Mitch (Kepert, 2006b), Danielle and Isabel (Schwendike, 2005) similarly show a consistent spatial variation of wind profile shape within each storm.

Several of the theoretical studies, reviewed below, have predicted that the upper boundary layer jet is supergradient. Balance in this situation has been analysed by Kepert (2002c, 2006a,b) and Schwendike (2005). They found that Hurricanes Mitch (1998) and Isabel (2002) had azimuthal-mean jets that were ~15% supergradient, but that Georges (1998) and Danielle (1998) did not. These differences highlight the inter-storm differences mentioned above, and are discussed further below.

Several studies have discussed boundary layer (BL) asymmetries due to proximity to land. Here, the higher roughness over land induces increased inflow, which is typically dryer, and produces a flow asymmetry that may extend into the eyewall. Analyses of these phenomena have been presented for Hurricanes Bonnie (Schneider and Barnes, 2005), Danny (Kepert, 2002a), Floyd (Kepert, 2002b) and Mitch (Kepert 2006b). This issue is discussed in more detail in topic 0.2.

Boundary-layer thermodynamics was analysed along inflow trajectories in Hurricane Bonnie (1998) by Wroe and Barnes (2003). They found little increase in inflow θ_e to within about 1.5 times the RMW, despite surface fluxes of over 500 W m^{-2} , since fluxes through the top of the BL, including those due to convective cells, remove moist entropy from the BL at the same rate as the sea supplies it. Inwards of this, the storm secondary circulation suppresses convection while the surface fluxes continue to increase, giving an increase in θ_e . To achieve balance, they found it was necessary to either allow for some entrainment through the BL top, or for dissipative heating. The energetics of the BL are of prime importance, in light of the considerable sensitivity of storm intensity to the energy content of the BL air beneath the eyewall.

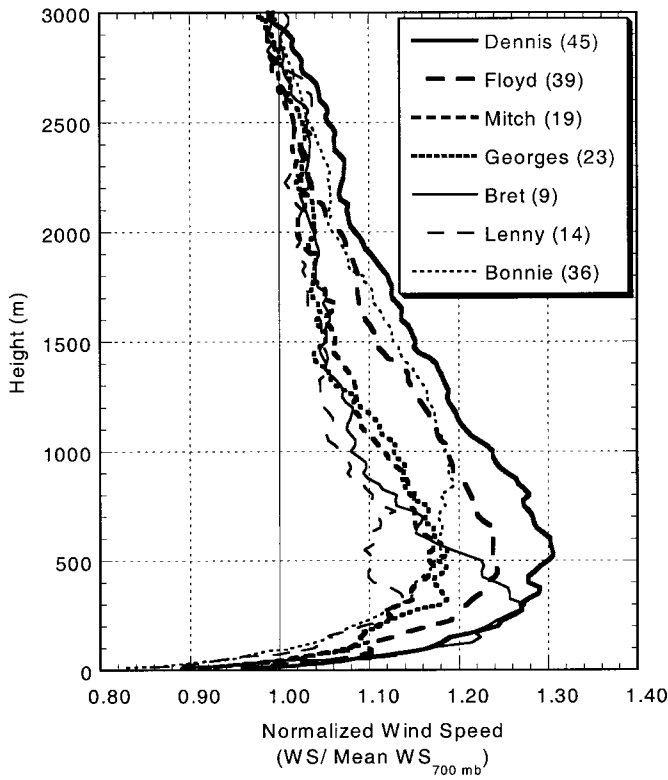


Figure 1.2.1. Mean observed eyewall wind speed profile in seven hurricanes, normalised by the wind speed at 700 hPa. From Franklin et al. (2003).

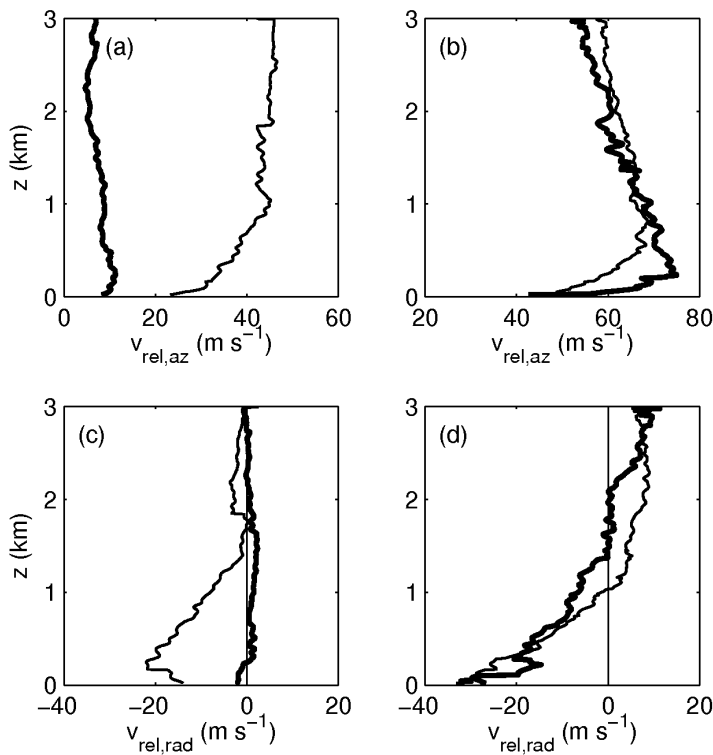


Figure 1.2.2. Observed wind profiles in Hurricane Mitch (1998). (a) Mean profiles of storm-relative azimuthal wind over radius ranges 0 – 15 km (heavy) and 40 – 100 km (light). (b) As for (a), over radius ranges 15 – 25 km (heavy) and 25 – 40 km (light). (c, d) As for (a, b), but for the storm-relative radial wind component. From Kepert (2006b).

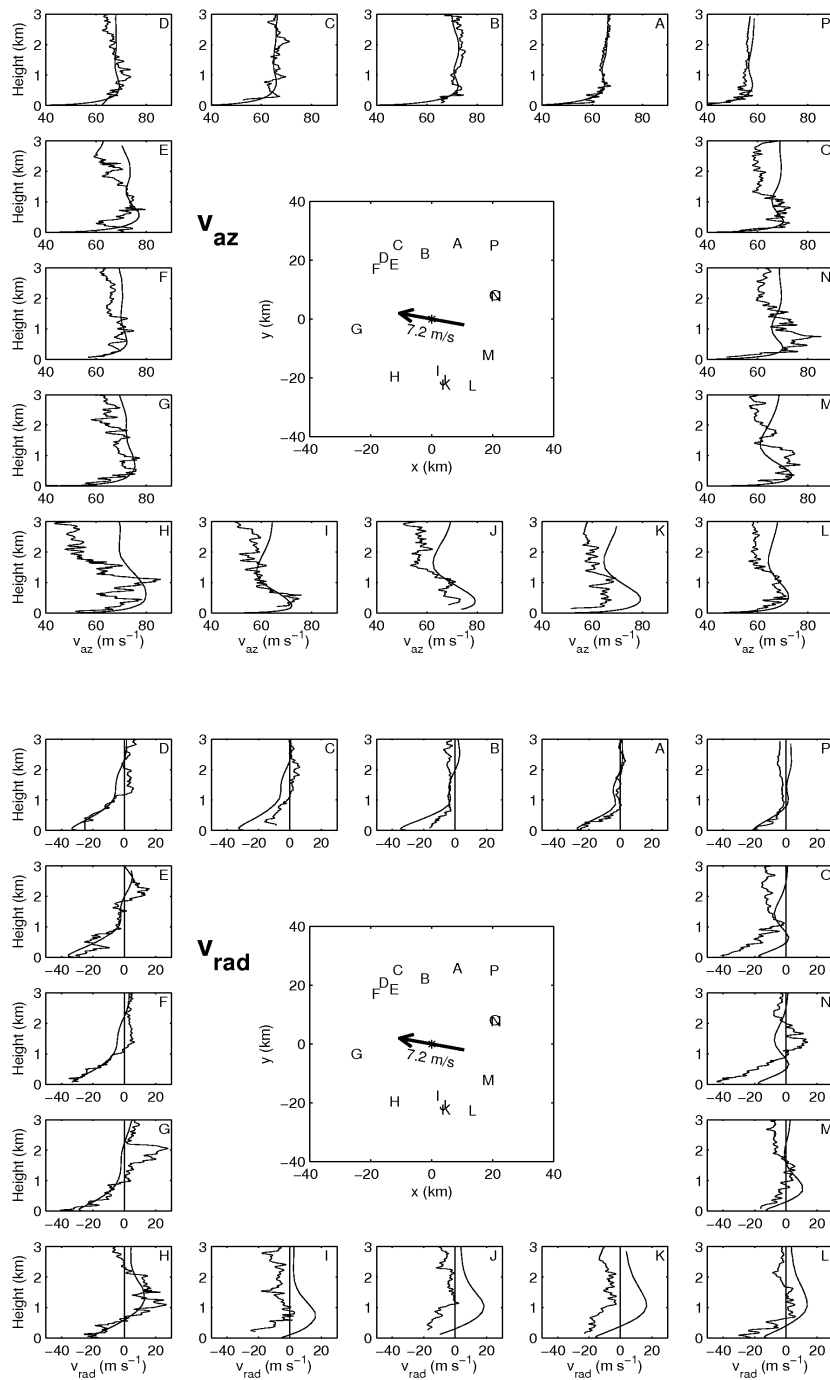


Fig 1.2.3: Profiles of the storm-relative azimuthal and radial wind components observed by dropsondes (curves with small-scale fluctuations) and represented in the model (smooth curves) in and near the eyewall of Hurricane Georges (1998). The model values were interpolated from the model grid to the observed dropsonde trajectory. The storm-relative position of each sonde as it fell through a height of 1 km and the storm motion are shown in the central panel. From Kepert (2006a).

b) Theory and Modelling

A satisfactory theory of the TCBL is thus challenged to explain the structure variation between storms, and with radius and azimuth within an individual storm. Idealised models of the TCBL date back to the 1960's and beyond (see the review in Kepert 2002c, Chapter 1). Their dimension serves to broadly classify them: 1-D column (e.g. Moss and Rosenthal, 1975; Powell, 1980), 1-D depth-averaged axisymmetric (e.g. Smith, 2003), 2-D axisymmetric (e.g. Rosenthal, 1962; Kuo, 1971, 1982; Eliassen and Lystad, 1977; Mallett, 2002; Montgomery et al. 2001), 2-D depth-averaged (Shapiro, 1983), and 3-D (Kepert, 2001; Kepert and Wang, 2001).

Several of the 2-D axisymmetric models, and the 3-D models, display low-level wind maxima. These have much in common with the observations; the azimuthal maximum is contained within the frictional inflow layer, the maximum becomes more marked towards the centre of the storm, and the depth of the BL decreases towards the centre of the storm. This last property is because the BL depth varies inversely with the square root of the inertial stability (Rosenthal, 1962; Eliassen and Lystad, 1977; Kepert, 2001). These authors show that the TCBL is a modified Ekman spiral, in which the inertial stability parameter l replaces the Coriolis parameter f , and the spiral is "stretched" in the cross-stream direction by a factor $((f + 2V/r)/(f + V/r + dV/dr))^{1/2}$. Here, the upper-BL wind maximum is similar to that in the Ekman spiral, and a few percent supergradient in these simple models.

These simpler models ignore the influence of vertical advection; including this process gives a markedly more supergradient wind maximum. Analysis of the momentum budget equations shows that the supergradient flow is generated by inwards advection of absolute angular momentum. The inflow is ultimately frictionally generated, but is maintained at the jet height against the outwards acceleration due to gradient imbalance by diffusive and advective transport from below; thus it is stronger in a model that contains vertical advection (Kepert and Wang 2001). Kepert (2006b) further relates this effect to the Ekman-like solution. If the vertical advection is zero or neglected, the oscillation and decay length-scales in the Ekman-like solution are equal. Introducing vertical advection makes these scales unequal; in an updraft, the oscillation scale is longer than that for decay, while in a downdraft the opposite applies. Thus the height-variation of the flow will exhibit larger oscillations near the BL top in an updraft than in a downdraft. This effect is strongest where upwards motion is strongest, so the BL jet is most marked beneath the eyewall and near rainbands.

The height-resolving 2-D and 3-D models generally show an increase in the SWF towards the centre of the storm; in fact, such predictions preceded the observations of this phenomenon. The depth-averaged axisymmetric and 2-D models show a similar increase in the relative strength of the BL-mean wind towards the centre. In both cases, this is due to advection of angular momentum by the frictional inflow maintaining relatively stronger near-surface winds than in BLs with straight flow, and the effect is strongest where both the inflow and radial gradient of angular momentum are strong; that is, near the eyewall (and possibly also near strong convective updrafts). It is important to note that these models do not include any enhancement of the turbulent transport by moist convection, but that the effect is purely dynamical. Thus Franklin et al's (2003) explanation for the reason for the observed SWF increasing towards the core and in areas of convection is likely incorrect.

Having established that radial advection plays an important role in shaping the structure of the axisymmetric BL, it is perhaps not surprising to learn that azimuthal advection also has a strong influence. Kepert (2001) showed that the motion-induced asymmetry has the horizontal structure of a wavenumber-1 inertia wave. Such waves normally propagate, with the phase speed varying rapidly with radius and are not observed. However, the effect of vertical diffusion is to retard the wave propagation: the vertical tilt (in azimuth) of the phase lines and decay of the wave amplitude adjust so as to bring the wave to a halt, locked in position with the asymmetric friction forcing it at the surface. There are two such waves, corresponding to the anticyclonically- and cyclonically-propagating inertia waves, but the stalled version of the anticyclonically-propagating one dominates. It rotates

anticyclonically with increasing height, and has a depth scale several times that of the symmetric component. Kepert and Wang (2001) used a numerical model to relax some of the assumptions in Kepert's (2001) analytical model, and also presented budget analyses that emphasised the role of horizontal advection in creating the spatial variation in BL wind structure. The inclusion of nonlinear processes, including vertical advection, tended to strengthen the jet, as in the axisymmetric case.

This stalled wave structure, when combined with the symmetric component, is able to explain several well-known features of the TCBL. In the northern hemisphere, the surface earth-relative wind maximum is in the right forward quadrant, and the inflow angles are greatest on the right of track and least on the left. It also predicts the more recent observational findings, including that the BL jet is more marked, more strongly supergradient, and closer to the surface on the left of track, and that the SWF is higher on the left than on the right.

These higher-dimension models demonstrate an important fact: that the TCBL, unlike much of the rest of the atmospheric BL, cannot be satisfactorily understood by 1-D, horizontally homogeneous (i.e., column) models. Rather, radial advection of angular momentum by the frictional inflow and asymmetric frictional forcing play a crucial role in determining the BL structure and depth.

Variations in angular momentum advection play an important role in determining the spatial variation in TCBL wind profile structure. The radial gradient in angular momentum varies greatly between storms – some storms have relatively “flat” radial variation in the wind strength, or equivalently, are inertially stable and have a radial gradient of angular momentum throughout, while others have “peaked” profiles, and are inertially near-neutral with weak angular momentum gradient outside the RMW. Kepert and Wang (2001) presented model calculations of the resulting BL structure for these extremes. The “flat” case had a weakly (5 – 10%) supergradient jet extending from the RMW to large radii, while the “peaked” one had a strongly (25%) supergradient jet confined to the vicinity of the RMW. The frictional inflow and eyewall updraft are also relatively stronger in the “peaked” case. Observational confirmation of these differences has been provided by Kepert (2006a,b) and Schwendike (2005), who found that of four storms analysed (Danielle, Georges and Mitch of 1998, and Isabel of 2002), two had markedly supergradient flow in the upper BL beneath the eyewall, and two were indistinguishable from balance. The difference in the structure of these storms is as predicted by Kepert and Wang (2001): the “peaked” storms had supergradient flow, while the “flat” ones didn't. Fig 1.2.3 contains the modelled wind profiles in Georges corresponding to the dropsonde observations, and shows that the model is able to reproduce much of the around-storm variation in structure, in both the azimuthal and radial flow components. Thus these analyses provide strong confirmation of the theoretical predictions, being able to explain not just the general features, but also the differences between storms.

Further evidence of the ability of these models to predict the differences between storms was provided by Kepert's (2004) preliminary analysis of the eyewall wind profiles discussed by Franklin et al. (2003). The Kepert and Wang (2001) model, forced by aircraft observations of radial storm structure, and combined with a crude calculation of the baroclinic warm core effect, was able to largely reproduce these differences. Thus the difference in “character” of eyewall wind profile between storms noted by Franklin et al. (2003), is seen to have a dynamical cause.

c) Stability Effects

Stability is known to have a profound influence on the atmospheric BL. Richardson number-based arguments show this effect will be smaller in the TCBL than elsewhere, but not absent. Powell and Black (1990) demonstrate that it is indeed important, producing a variation in the observed SWF of ~0.1, of similar magnitude to the dynamical variations discussed above. Little further work has been done on this factor, but it is clearly important to a complete understanding, and the ability to accurately predict, the TCBL flow.

d) Operational Implications

Theoretical predictions of spatial variation in the SWF, supported by observational analyses, have led

to changes in the way aircraft-observed winds are used to estimate the surface wind. This has resulted in an increase in the estimated intensity of storms with aircraft reconnaissance, and to the reanalysis of historical storms to higher intensity, such as Hurricanes Andrew (Landsea et al., 2004) and Donna (Dunion et al., 2003). This increased knowledge will also impact in storm analysis when aircraft reconnaissance is not available, since analysis of such storms rests heavily on the Dvorak technique (see Velden et al. 2006 for a review), which is calibrated against aircraft data.

There are also implications for areas such as central pressure – maximum wind relationships, and the formulation of parametric wind models used for forcing storm surge and wave models, and for engineering and insurance risk analyses.

One missing factor in such applications is the effect of eyewall slope. The eyewall is approximately an angular momentum surface, thus the maximum gradient wind will vary little with height along a near-vertical eyewall, but will increase towards the surface when the eyewall is sloped away from the vertical. Little information is available about the impact of this, although Dunion et al. (2003) present a statistical scheme that includes this effect. Kepert (2004) shows how to calculate the slope of the angular momentum surfaces from flight-level wind and temperature data under certain assumptions and uses this to calculate the surface pressure field. The derived surface pressure field (and storm motion) may then be used to force the Kepert and Wang (2001) model to account for the effect of friction.

1.2.2.2 Transients and Instabilities

The TCBL supports a number of instabilities and transient structures. There is some overlap between this topic and that of general instabilities leading to spiral band structures. This section considers phenomena that are clearly part of the BL, chiefly rolls. There have also been several reported cases of fine-scale spiral bands reported in the TCBL, which are larger in scale than the above cases and so it is not clear that they are the same phenomenon. Examples include Gall et al. (1998), Kusunoki and Mashiko (2006), Kusunoki (2006). The reader should refer also to the discussion in section 1.2.4.2 for fine-scale spiral bands that occur partly within the BL.

a) Boundary Layer Rolls - Observations

Boundary-layer rolls are very common in the atmospheric BL (see e.g. Etling and Brown 1993 for a review). Wind circulations associated with these rolls can produce highly organized and damaging surface winds (Wakimoto and Black 1994). Wurman and Winslow (1998) presented the first Doppler radar evidence for their existence in tropical cyclones, indicating intense horizontal roll vortices with an average wavelength of 600 m roughly aligned with the mean azimuthal wind in Hurricane Fran near landfall. The associated variation of wind speed was large: bands of 40 – 60 m s⁻¹ flow alternated with 15 – 35 m s⁻¹. Several papers have since presented similar evidence. Katsaros et al. (2002) examined SAR images of Hurricanes Mitch and Floyd and also found periodic kilometre-scale variation. More recently, Morrison et al. (2005) describe features that are significantly less streaky in appearance, to the extent that it is not entirely clear that they are the same phenomenon. The different radar technology used by the groups may have contributed to this difference.

Lorsolo et al. (2006) analyse the vertical structure of the rolls, find them to be coherent through the depth of the BL (~500 m), and compare radar- and tower-measured winds with good agreement, demonstrating that the roll circulation extends to the surface, albeit with other scales of motion superimposed.

b) Boundary Layer Rolls – Theory

Theoretical analyses of roll development in tropical cyclones were provided by Foster (2005) and Nolan (2005). Foster (2005) argues that the tropical cyclone BL is an ideal environment for roll development. His argument extends the classical theory of roll development as an inflection-point

instability of the frictionally-induced cross-isobar flow to the case of a tropical cyclone. Here, the cross-stream shear and hence instability are strong because the BL is relatively shallow, and the cross-stream component in analytical solutions is stronger than in classical Ekman-like solutions for straight flow (Kepert 2001). Nolan (2005) presents a stability analysis of a symmetric vortex, and finds both symmetric and asymmetric responses. The instabilities acquire some energy from the shear in the radial flow near the top of the BL, in which regard they are similar to Foster's (2005) rolls. However, Nolan shows that the vertical shear of the azimuthal wind can also contribute energy to the instability, and that the relative importance of these mechanisms depends on the inertial stability of the storm and on the orientation of the mode.

c) Turbulence and Gusts

The GPS dropsonde has now been operational for close to a decade, and several thousands have been deployed in the eyewall of hurricanes. Extreme gusts have been reported in both horizontal and vertical wind components (Aberson and Stern 2006, Henning 2006, Stern and Aberson 2006). While these are (by definition) rare events, the steadily increasing sample is beginning to enable statistical characterization of their nature.

Specially-deployed towers have been used in landfalling hurricanes for several years, and are yielding valuable data on the turbulence structure. Schroeder and Smith (2003) calculated a range of turbulence statistics from data taken during the landfall of Hurricane Bonnie, and found general agreement with established gust factor curves, but additional energy in the power spectrum at low frequencies.

Wind averaging periods continue to differ between operational centres, with conversion and interpretation presenting problems. Problems include with the calibration of the Dvorak technique, usually taken to provide a 1-minute mean wind speed, for use in centres which employ 10-minute averaging.

d) Other small-scale features in the boundary layer

Analyses of dropsonde wind data in Hurricane Georges (1998), shown in Fig 1.2.4, reveal a distinct wavenumber 3 asymmetry in the flow near the eyewall below 1 km (Kepert 2006a), which was apparently not propagating and persisted for the period of the observations (6 hours). The lack of propagation and shallow depth rule out all known TC instabilities as a cause – in particular, these are distinct to the usual eyewall mesovortices discussed in section 1.2.3.2. A similar feature, except at wavenumber 2, was seen in the BL beneath the eyewall of Hurricane Humberto (2001) (S. Feuer, personal communication, 2003).

e) Operational Implications

Observations and theory show that BL rolls are common in TCs, and are associated with streaks of strong winds at the surface. The presence of these coherent structures implies that wind damage will be different to that expected in a "more random" turbulent field. They may also result in more efficient transport of heat, moisture and momentum than is presently assumed in numerical models of TCs.

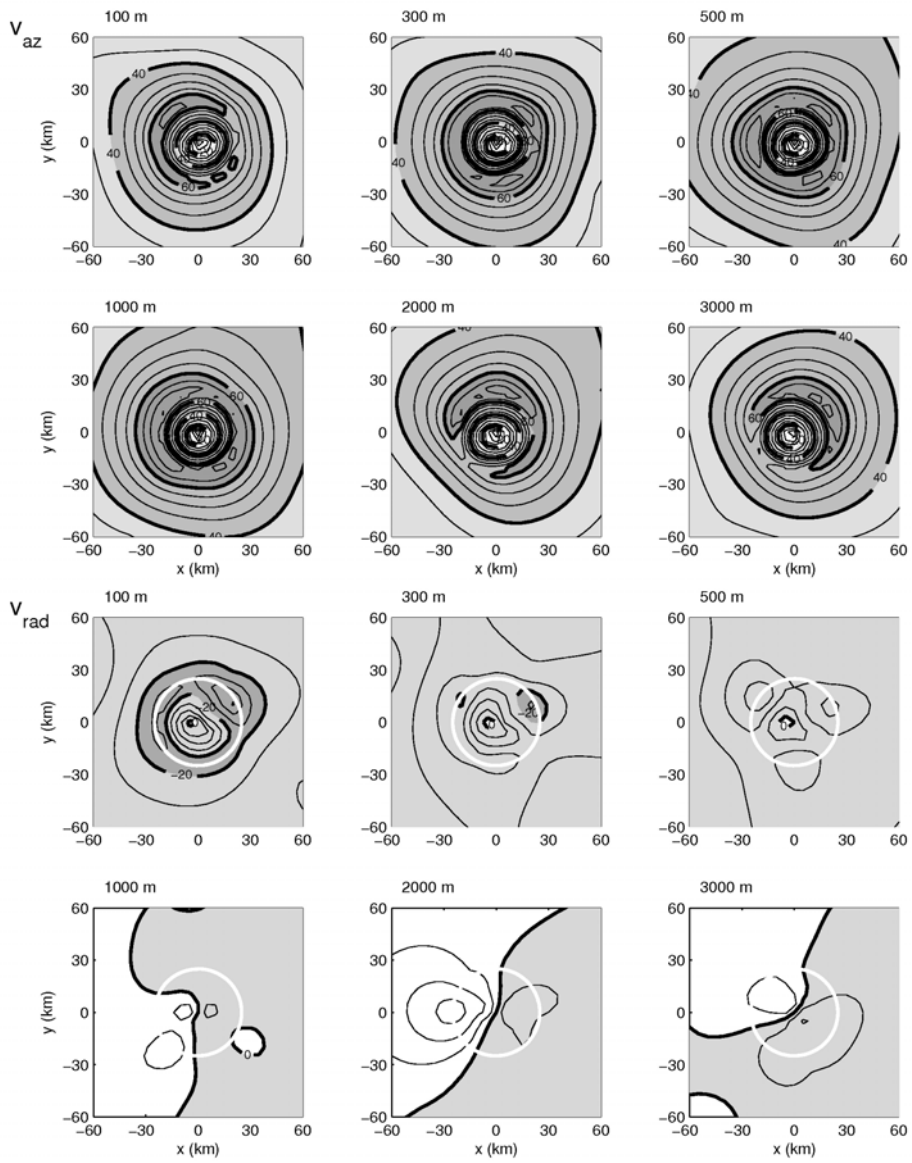


Fig 1.2.4. Analyses of the storm-relative azimuthal (upper 6 panels) and radial (lower 6 panels) wind component at several levels in Hurricane Georges (1998). The contour interval is $5 m s^{-1}$ with heavy labelled contours at multiples of $20 m s^{-1}$. Darker shading corresponds to stronger winds (upper panels) and stronger inflow (lower panels). The white circle in the lower panels indicates the approximate RMW. From Kepert (2006a).

1.2.3. The eye and eyewall

Tropical cyclone (TC) intensity change is governed by a number of known factors. The climatology of intensity change was documented by Dvorak (1984) and showed that an average tropical storm intensifies at a rate of a few m/s per day, and an average hurricane intensifies at a rate of about 12 – 13 m/s per day. This mean intensity change typically continues for 3 – 5 days after the storm reaches tropical storm strength (18 m/s). After maximum intensity, weakening typically occurs at a slower rate. This was recently corroborated and expanded by Emanuel (2000) who showed that a storm that does not encounter land or decreasing sea surface temperatures, intensifies, on average, at a rate of about 12 m/s per day for about 5 days, and then begins to weaken at a slower rate of about 8 m/s per day.

In addition to the climatology of intensity change, we also know that environmental conditions play a key role – for example, if a storm moves over colder water or land, or if the ambient environmental vertical wind shear increases, weakening typically follows. Alternatively, an environment that is not conducive for intensification can become more favorable over time, and strengthening would typically occur. Ideally then, we would be able to explain the variance from climatology of hurricane intensity change in terms of the variance of the synoptic-scale storm environment. This is not the case however, and it is fairly typical for storms to strengthen or weaken, sometimes rapidly, without any commensurate changes in the external storm environment. Although the specific processes involved remain an open question, this behaviour is widely believed to result from internal vortex-scale processes that can have a profound effect on how storm intensity evolves, and this means that our ability to model and ultimately predict hurricane intensity change is dependent on our ability to simultaneously model a very broad range of spatial scales.

The vortex-scale processes to be considered include PV redistribution resulting from dynamic instability of the eyewall and PV transport by mesovortices, eyewall replacement cycles, and mean-flow amplification via PV.

1.2.3.1 Symmetric structure

a) Eyewall Contraction, Expansion and Replacement

The most remarkable eyewall process related to TC intensity change is the concentric eyewall and eyewall replacement processes (Willoughby et al., 1982). In this concentric eyewall model, as a TC and its primary eyewall intensifies, convection outside the primary eyewall becomes organized into a ring (the secondary eyewall) that encircles the inner eyewall and coincides with a local tangential wind maximum. As the second eyewall propagates inward and amplifies, the inner eyewall weakens and is eventually replaced by the outer eyewall. This eyewall replacement cycle is usually accompanied by a weakening and then a re-intensification of the TC; and thus producing a large fluctuation in TC intensity. While this process is well known, recent years have seen a substantial increase in our ability to monitor it, which we now review.

Tropical cyclone (TC) eyewalls have been under sampled by visible/IR imagery due to persistent upper-level cloud obscuration. However, satellite microwave sensors can “see through” non-raining clouds (Spencer et al., 1989) and thus have unraveled several TC inner-core secrets by providing “snapshots” depicting eyewall evolutions (Hawkins et al., 2006). In addition, two new microwave imagers (SSMIS and WindSat) since IWTC-V have augmented the temporal sampling from these polar orbiter-based sensors and enhanced our knowledge of eyewall characteristics.

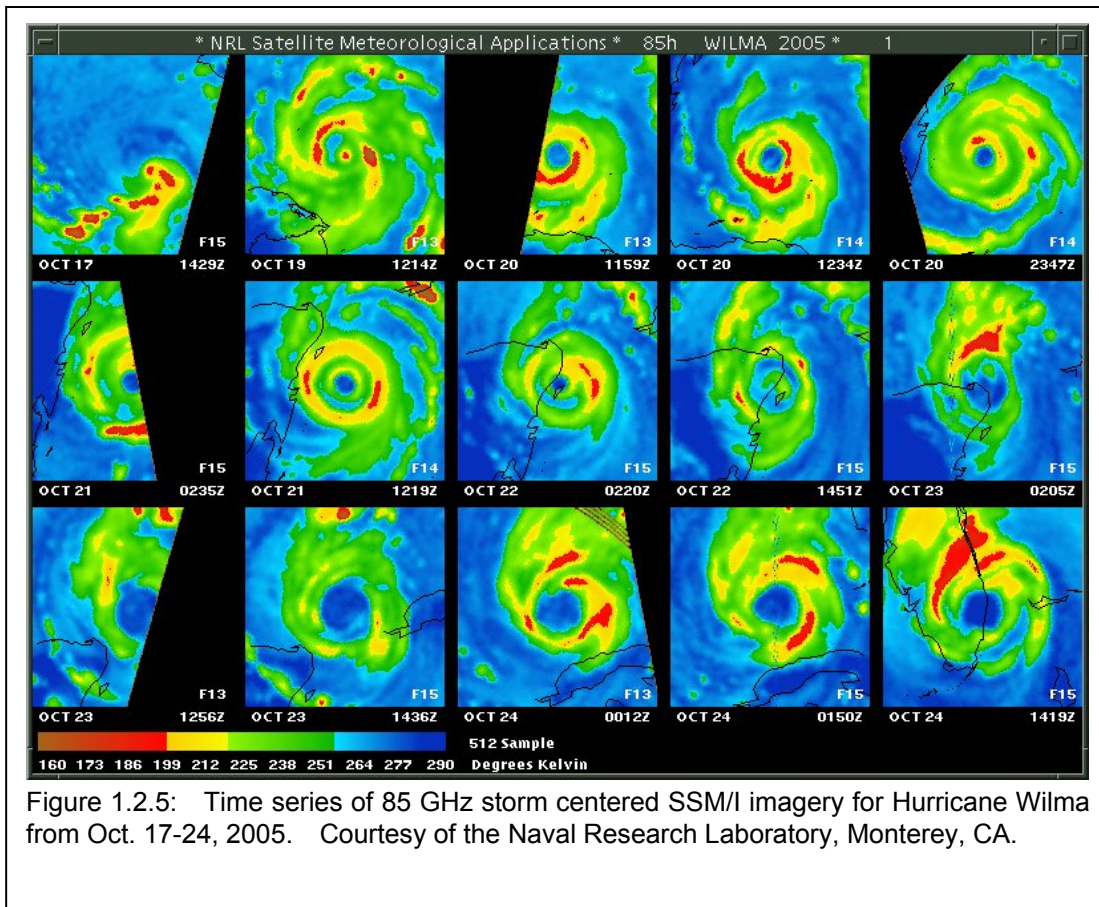
The ability to “see through” non-raining clouds permits satellite analysts to more accurately monitor inner-storm structure that perplexes vis/IR imagery such as: a) early eyewall formation, embedded eyes, middle and upper-level shear and concentric eyewalls (Hawkins et al., 2001). TC multiple eyewall characteristics have been outlined in a growing number of papers as noted by Hawkins et al. (2006), McNoldy (2004), Kodama and Yamada (2005), Hawkins and Helveston (2004), an excellent

summary by Simpson et al. (2003), Lee et al. (2002), and Velden and Hawkins (2002). Each effort utilizes microwave data sets to view and infer eyewall configurations.

Currently, a constellation of “operational” and research passive microwave imagers and sounders provide sufficient temporal coverage to capture many eyewall structure changes. The four operational imagers include the Special Sensor Microwave Imager (SSM/I, Hollinger, 1989) and the Special Sensor Microwave Imager Sounder (SSMIS, Wessel et al., 2003). A wealth of research instruments greatly aids these sensors: the TRMM Microwave Imager (TMI), the Advanced Microwave Scanning Radiometer (AMSR-E), and the Coriolis WindSat polarimetric radiometer. This suite of seven (7) microwave imagers will not likely be repeated for decades based on future global launches (National Research Council, 2004, 2006). Coarser resolution microwave sounders also help map eyewall/rainband features: the Advanced Microwave Sounding Unit (AMSU-3) and the Microwave Humidity Sounder (MHS-1). These four operational cross-track scanners are best at nadir and can assist with storms having normal or large eyewalls.

TC eyewalls form as the result of rainbands spiralling into the system centre and eventually organize into a continuous circular-like band of enhanced convection. The beginning eye diameter can have a huge range in values, but eyewall diameter typically decreases as the storm intensifies. Eyewall contraction continues and reaches a “minimum” diameter at peak strength. Many storms begin formation of a secondary eyewall at a larger radius once the inner eye reaches a critical diameter. This formation process most frequently occurs at 120 kts or higher. The secondary eyewall completely encircles the inner eye, moisture and momentum flux to the inner eye declines and it decays, eventually leaving only the outer eye at a much larger radius than the first eyewall. The secondary eyewall (now main eyewall) can contract inward and begin the process again (eyewall replacement cycle-ERC). ERCs can continue for two or three times depending on environmental characteristics and are most likely to occur within western Pacific typhoons that form in the deep tropics near Guam and don't encounter strong shear or cold SSTs (Hawkins et al., 2006).

The eyewall replacement cycle was captured for Hurricane Wilma as illustrated in storm-centred 85 GHz imagery in Fig 1.2.5 (Hawkins et al., 2006). During a one week timeframe, the storm formed a single eyewall (Oct 20th) that transitioned to two eyewalls by Oct 21st as a major rainband spiralled in from the SW sector, and the small inner eyewall decayed by the 23rd as the outer eyewall become the remaining eyewall feature. The new eyewall retained its large diameter as the storm raced across south Florida, largely explaining the extended area of high damaging winds. If favourable conditions persist (warm SSTs, weak shear, no trough interactions, etc) the process can repeat, but it was interrupted by landfall and a strong trough in Wilma's case.



Studies of nine years of passive microwave data reveal that 40-80% of TCs reaching 120 kts or higher obtain double or concentric eyewalls (Hawkins et al, 2006). The southern hemisphere has the lowest percentage (40%), eastern Pacific (50%), Atlantic (70%) and western Pacific (80%). These values fluctuate markedly from year to year and basin to basin, but more intense storms (Cat 3 and higher) have the greatest chance to form and maintain double eyewalls. The duration of double eyewall configuration can range from less than 12 hours to 2-3 days and is directly dependent on environmental conditions. For example, shear can stop double eyewalls in short order.

A few intense double eyewall storms do not follow the typical eyewall replacement scenario, but instead form a wider single eyewall with extremely cold cloud tops (IR) and brightness temperatures (Tb- microwave). In addition, rainbands tend to dissipate or become significantly shortened as the TC takes on an “annular” outline (Knaff et al., 2003). These annular storms exist in specific shear and SST regimes, and can maintain their intensity for multiple days with maximum sustained winds in excess of 120 kts. Efforts are currently underway on automated methods to help predict which TCs will evolve into annular and concentric eyewall systems since they represent key forecast busts as the MSLP for annular storms are typically under forecast while concentric TCs are over forecast (Kossin et al., 2006; Cram et al., 2006).

The initiation of concentric eyewalls has been studied in idealised models by Nong and Emanuel (2003), who show that the wind-induced surface heat exchange (WISHE) instability is necessary for their growth. They argue that a finite-amplitude, externally forced perturbation is necessary to trigger the instability, and that the growth is sensitive to the boundary-layer moisture. This will make prediction challenging, as this parameter is often poorly observed over the tropical oceans. Recently, Cangialosi

et al. (2006) and Ortt and Chen (2006) reported success in a couple of cases of outer eyewall formation prediction, using high-resolution NWP in research mode.

b) Inner-core buoyancy

Recent numerical studies (Zhang et al. 2000, Braun 2002) and aircraft flight-level data analysis (Eastin 2002, 2003) show different results regarding the relative role of buoyancy and perturbation pressure gradient forces near the core and eyewall of tropical cyclones (TCs). In a numerical simulation of Hurricane Andrew (1992), Zhang et al. concluded that air in the eyewall was negatively buoyant and was forced upward by perturbation pressure gradient forces. However, in a similar simulation of Hurricane Bob (1991), Braun found that eyewall updrafts are positively buoyant with respect to an environment that includes the vortex-scale warm-core structure. Eastin examined the buoyancy of eyewall convective updrafts in hurricanes based on aircrafts flight-level reconnaissance data and found that eyewall updraft cores were positively buoyant relative to a background mesoscale environment.

Smith et al. (2005) established a generalized buoyancy force with the basic state as a function of height and radial distance. The buoyancy can be distinguished as one part related to the symmetric balanced vortex (system buoyancy) and the other part associated with cloud dynamics (local buoyancy). They suggested that the discrepancy of the foregoing studies is mainly a result of different definition of the buoyancy, in particular, its reference states. In Zhang et al., a reference state that varies in time and space was obtained by performing a running mean of the numerical model output over four neighbouring grid points on a constant σ -surface. In contrast, Braun used Fourier decomposition into different azimuthal wavenumbers and selected wavenumbers 0 and 1 to define the reference state. These two representations are more akin to the local buoyancy defined by Smith et al. (2005). Eastin defined the reference state by applying a running low-pass (Bartlett) filter to data along the flight track. This method corresponds more with the definition of the local buoyancy. Although the buoyancy force may be different when derived from different reference states, the sum of the buoyancy force and the perturbation pressure gradient is unique, and it is the sum that determines the vertical motion. In addition, results from both Braun and Eastin indicate that although the updrafts associated with positive buoyancy covers only a small portion of the eyewall area, they account for a majority the upward mass flux, consistent with the concept of “hot towers” (Hendricks. et al. 2004).

Zhu and Smith (2002) explained the mechanism of shallow convection in stabilizing the core region of a TC. The shallow convection transports air with low moist static energy from the lower troposphere to the boundary layer, stabilizing the atmosphere not only to itself, but also to deep convection and reduces the rate of heating and drying in the troposphere. Also it moistens and cools the lower troposphere. This reduced heating, together with the direct cooling of the lower troposphere by shallow convection, diminishes the buoyancy in the vortex core and thereby the vortex intensification rate.

Regarding the structure of the buoyancy, Eastin et al. (2005a,b) further examined the buoyancy distribution in the inner core of Hurricanes Guillermo (1997) and Georges (1998) using airborne radar, dropwindsonde, and flight-level observations. Their results indicate that the low-level eye can be an important source region for buoyant eyewall convection. It was observed that buoyant eyewall updraft cores and transient convective-scale reflectivity cells are predominantly downshear and left-of-shear. Most eyewall downdraft cores that transport significant mass downward are located upshear. Negative buoyancy was most common in left-of-shear downdrafts, with positive buoyancy dominant in upshear downdrafts. Some buoyant updraft cores were encountered in the midlevel eyewall exhibit equivalent potential temperatures much higher than in the low-level eyewall, but equivalent to the observed in the low-level eye. Asymmetric low-wavenumber circulations appear to be responsible for exporting the high- θ_e eye air into the relatively low- θ_e eyewall and generating the locally buoyant updraft cores. It was suggested that an ensemble of asymmetric buoyant convection could contribute to hurricane evolution possibly with three different mechanisms.

While the “hot towers” concept is popular recently in explaining the development of TC through a two-stage process (Hendricks et al. 2004), it appears that more studies may be needed to understand

the asymmetric buoyancy distributions during a decaying as well as an intensifying stage to understand the thermodynamics associated with.

c) Parametric Representation

Many practical applications require a simple representation of the surface wind field of a TC, dependent on only a few parameters. Examples include storm surge modelling, risk analysis, and engineering design. Of the several extant, the parametric profile of Holland (1980) has been most widely used for such applications, usually with an ad hoc representation of the motion asymmetry and boundary layer friction added.

The Holland profile has several deficiencies, including that the wind maximum is insufficiently sharp, and that the decay of wind speed at large radius may be incorrect (Willoughby et al., 2004). A new family of profiles (Willoughby et al. 2006) overcomes these problems, although at the cost of having more free parameters, and being less tractable mathematically.

Mallen et al. (2005) studied the radial profile of vorticity using aircraft data and showed that some parametric profiles are deficient, in that they may have an annulus of negative relative vorticity. Such an annulus is not present in observations, while Reasor et al. (2004) discuss theoretical reasons for its absence being important for the ability of the vortex to resist shear. Although Mallen et al. did not consider the Holland (1980) and Willoughby et al. (2006) profiles, the former always has this problem, while the latter may if parameter values are not carefully chosen.

Many applications require near-surface winds, while the profiles deliver a gradient-level wind. Crude ad hoc parameterisations of friction and the motion-induced asymmetry are customarily used. The analytical boundary-layer model of Kepert (2001) would seem to offer advantages here, since it includes much of the relevant physics, but has so far not been widely adopted for this purpose.

d) Radar Observations

To be relevant, observations of the inner core region of a tropical cyclone need to be available at high temporal and spatial resolution. These requirements can be satisfied with radar. Doppler radar observations (ground-based or airborne) stand as powerful tools to capture the three-dimensional wind structure and reflectivity field. But the Doppler velocities can not be used immediately and need to be processed by some sophisticated algorithms to become interpretable. The VTD (velocity track display) method can retrieve the symmetric part of the tangential and radial wind (Lee et al., 1999; Lee and Marks 2000; Lee et al., 2000) and EVTVD (extended velocity track display) method can determine wavenumber-0 and -1 components of tangential and radial wind; this last one was also extended to ground-based radar by Roux et al, 2004 (GB-EVTVD: ground-based extended velocity track display). Recently, Liou et al. (2006) used two radars in a very similar method.

The GB-EVTVD technique has been applied to the intense cyclone Dina (Roux et al, 2004) when its elliptical cyclonically rotating eye passed closest (<130 km) to La Réunion island. The three-dimensional dynamical structure of the inner core region and structure of the rainbands is well seen and very instructive. The rotating maximum tangential wind is correlated to the presence of maximum reflectivity values. The steep orography of La Réunion affects the basic flow and the cyclone wind field as well which induces modifications in the internal structure of the cyclone. The maximum tangential wind migrates from east to south which can locally bring to very variable impact on such a small island; this information has therefore a great impact on the nowcasting.

Nuissier et al (2005) used airborne Doppler radar data to define a specified vortex for model initialization. They removed the ill-defined, too weak and misplaced vortex in global analyses (Kurihara et al., 1993, 1995) and replaced it by a balanced vortex deduced from airborne Doppler radar data.

1.2.3.2 Asymmetries of and inside the eyewall

a) Eyewall mesovortices

The existence of small vortices, of ~10km scale, abutting the inner edge of the eyewall, has been known for some time, and is associated with the occasional occurrence of a markedly polygonal structure of the inner edge of the eyewall on radar reflectivity images (e.g. Muramitsu 1986). These polygonal eyewalls had typically between 3 and 6 sides, and rotated somewhat more slowly than the azimuthal flow. Aircraft observations (Marks and Black, 1990; Black and Marks, 1991) showed that in extreme cases, an eyewall mesovortex (EMV) could be associated with local wind and pressure perturbations of magnitude approaching that of the primary vortex core. Recently, new observations and improved physical understanding has shown that these EMVs are quite common, represent an additional hazard to humanity, and play a role in the overall dynamics of the storm. A spectacular recent example was the six EMVs observed in Hurricane Isabel, shown in Fig 1.2.6 (Kossin and Schubert, 2005).

Kossin and Eastin (2001) used aircraft data to show that the wind and thermodynamic structure of strong TCs evolve between two distinct regimes. In regime I, the radial profile of wind across the eye is U-shaped, with maximum angular velocity within the eyewall, and an annular ring of vorticity just inside of the RMW. The eye is typically warm and dry, with elevated values of θ_e in the eyewall and lower values within the eye. Regime II, in contrast, is characterised by a V-shaped wind structure within the eye, with vorticity and angular velocity maxima near the centre of the eye. The air in the eye is relatively moist, with a θ_e maximum near the vortex centre. Transitions from regime I to II can be very rapid, occurring in less than an hour. The simultaneous change in kinematic and thermodynamic variables suggests the sudden onset of intense horizontal mixing between the eyewall and the eye. This mixing appears to be caused by the onset of eyewall mesovortices (EMVs), consistent with the barotropic instability of regime I. Kossin and Schubert (2003) discuss how this mixing is distinct from a horizontal diffusion process.

This barotropic instability is similar to that in other strongly sheared flows. The regime I hurricane is approximately a hollow tower of vorticity (located just inside of the RMW), with less vortical flow inside and out. Vortex Rossby waves can propagate on both high vorticity-gradient surfaces of the tower: on the inner face, the propagation is with (i.e. faster than) the flow, while on the outer face, it is against (slower). It is thus possible that the inner and outer waves can phase lock and mutually amplify, leading to exponential growth of the waves. This process was modelled in an unforced barotropic model by Schubert et al. (1999), who showed that the vortex ring could break down into several mesovortices, which subsequently merge to form a vortex monopole. Thus the wind profile went from U-shaped to V-shaped; precisely the change later noted in aircraft data by Kossin and Eastin (2001).

A range of final vortex structures is possible, depending on the size, width and strength of the initial vortex ring. Kossin and Schubert (2001) explore the part of the parameter space relevant to TCs. The typical response is for the vortex ring to break into a relatively large number of mesoscale vortices, which subsequently merge. These mergers may proceed to give a single discrete vortex monopole, or to a quasi-stable "vortex crystal", an asymmetric lattice of mesovortices rotating as a solid body. The flow associated with such a structure consists of near-straight line segments, making up a persistent polygonal shape. Such lattices can also undergo internal rearrangements – e.g. from a pentagon with a central mesovortex to a hexagon, and back again. The former of these structures is strikingly similar to the well-known instance of mesovortices in Hurricane Isabel (Fig 1.2.6).

These dramatic rearrangements of vorticity are accompanied (in the model) by equally spectacular pressure changes. In the change from the U-shaped (vorticity hollow tower) to the V-shaped (vortex monopole) structures, the winds inside the eye accelerate dramatically, while the maximum wind decreases. Integrating the gradient wind equation inwards (or solving a nonlinear balance equation),

the net effect is that the central pressure falls substantially, even while the intensity as measured by the strongest winds decreases.

Similar vortices have been produced in the laboratory. Montgomery et al. (2002) describe a water-flow apparatus which produces a curved shear layer, with primary and secondary circulations and aspect ratio similar to a hurricane. Two quasi-steady vortices, together with intermittent secondary vortices, form from shear instability of the curvilinear shear layer on the inner side of the “eyewall”. The peak tangential velocity occurred within the mesovortices, and was ~50% stronger than that of the parent vortex.

An eye structure, intermediate between the Kossin-Eastin regimes, associated with TCs with an unusually high degree of axisymmetry, was identified by Knaff et al. (2003) and named “annular hurricanes”, also known as “truck tyres” from their appearance on IR satellite imagery. These storms apparently form from the asymmetric mixing of eye and eyewall, possibly by mesovortices, but the mixing does not proceed all the way to the monopole structure of regime II. Annular hurricanes form within certain specific and relatively rare environmental conditions, including weak SE’ly environmental shear (in the Northern Hemisphere) and favourable thermodynamics, as measured by the potential intensity (PI). As well as the large and symmetric eye, they are also unusually symmetric outside the eye, with little evidence of outer rainbands. Significantly for forecasting, they maintain intensity longer and weaken more slowly than other TCs, and are thus a significant source of intensity forecast error.

Persing and Montgomery (2003) used an axisymmetric model to test the PI theory of Emanuel (1987, 1995). They found that, when run at high resolution, the model predicted intensity averaging about 20 m/s higher than PI, which they dubbed “superintensity”. The reason for this was that the model developed small-scale vortices, aligned with the mean flow, along the inner edge of the eyewall. These vortices efficiently mix the high- θ_e air from the eye boundary layer into the eyewall updraft, increasing the energy content of this air and hence the storm intensity. Although their model is axisymmetric and cannot generate EMVs, they argue that EMVs might similarly transfer high- θ_e air into the eyewall, a process that is absent from the derivation of the PI theory. In this context, Braun (2002) presented evidence of episodic mixing of eye air into the eyewall by EMV-like features, and also showed that θ_e was not constant along parcel trajectories in the eyewall, due to this mixing process.

Much of the interest in EMVs has been in highly symmetric storms with a clear eye in the cirrus overcast, since this facilitates their identification from satellite imagery. Recently, two studies (Braun et al., 2006; Halverson et al., 2006) have shown that they also exist in sheared storms, where the axis is tilted. A tilted axis is associated with enhanced low-level convergence and ascent on the downtilt side, leading to increased rainfall downtilt left (in the Northern Hemisphere). The opposite applies uptilt. These papers showed that EMV-like features may orbit the tilted eyewall, with their updraft and vorticity intensifying as they moved into the favourable downtilt area, and weakening as they leave it. Cyclonic advection of the enhanced convection in the EMVs lead, in the case of Hurricane Erin, to the coldest cloud tops being on the upshear side of the storm.

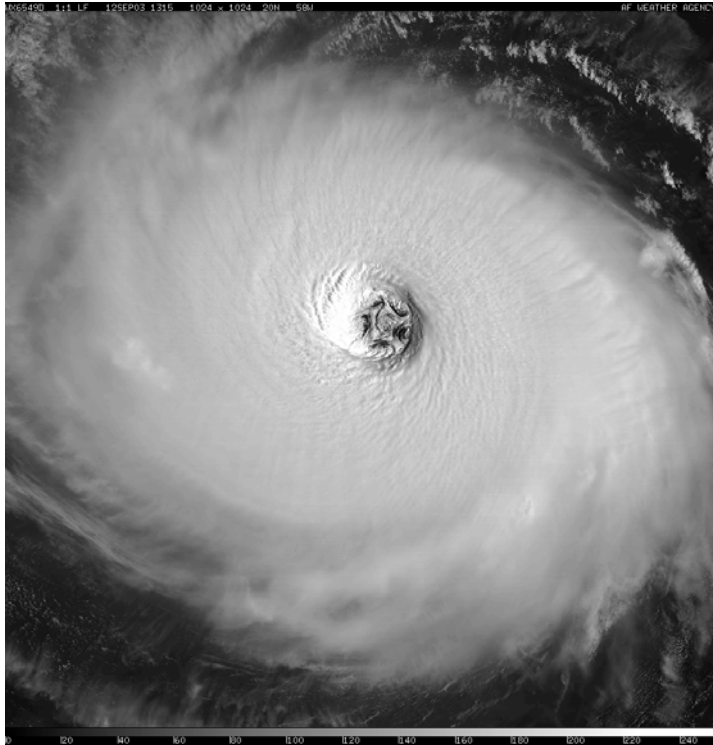


Figure 1.2.6: Defense Meteorological Satellite Program visible image of Hurricane Isabel at 1315 UTC 12 Sep 2003. The six mesovortices - one at the centre and five surrounding it - cause the starfish pattern in the eye.

b) Partial eyewalls

Another eyewall process is the so-called partial eyewall replacement proposed and studied numerically by Wang (2002b). He argued that strong perturbation from an outer spiral rainband could amplify the vortex Rossby waves in the eyewall, causing a large distortion of the eyewall and partial eyewall breakdown accompanied by a weakening of the TC. The eyewall can later recover from breakdown through axisymmetrization, resulting in a re-intensification of the storm. Therefore the eyewall breakdown/recovery is accompanied by a weakening/intensifying cycle of the TC. This partial eyewall cycle is an asymmetric process, and hence is different from the symmetric eyewall replacement studied by Willoughby et al. (1982). The latter is possible only for highly symmetric, intense storms, while the former can happen to both symmetric and asymmetric, and both intense and weak, storms.

1.2.3.3 Eye Tilt

There are quite different processes that can cause the eye of a tropical cyclone to tilt. The vertical shear of environmental flow in which the tropical cyclone is embedded is frequently cited as the major factor (e.g., Jones, 1995; Wang and Holland, 1996c; Frank and Ritchie, 1999; see also subtopic 1.1 report). Other processes include the so-called beta-effect (e.g. Wang and Holland 1996a, b), and interaction with another tropical cyclone or synoptic/mesoscale systems (e.g. Wang and Holland, 1995; Holland and Lander, 1993). The tilt of the inner core structure has many consequences. It complicates the interaction between the tropical cyclone and its large-scale environment because the tilted vortex involves self interaction between the upper and lower levels. Understanding the dynamics of a tilted vortex is thus as equally important as the interaction with large-scale environment.

Since the atmosphere on the rotating earth is vertically stratified, any perturbation, such as a potential vorticity (PV) anomaly, on one layer can have an impact on the other through the so-called vertical penetration (Hoskins et al. 1985) or vertical coupling. As a result, a self interaction of a tilted vortex may be expected and the extent to which the interaction occurs depends strong on a so-called vertical penetration depth, which is a function of the horizontal scale of the vortex and the background

stratification and local rotation (Shapiro and Montgomery 1993). The first-order interaction of the tilted tropical-cyclone-like vortex is the mutual cyclonic rotation of the upper and lower vortex centres due to the vertical penetration flow associated with the inner-core PV anomalies. Given an initially tilted cyclonic vortex without any environmental flow on an f -plane, the surface vortex centre would experience a cyclonic looping motion (Smith et al., 2000; Reasor and Montgomery, 2001). Even with constant vertical shear forcing, the track wobbles or oscillations can be expected (Jones, 1995; Wang et al., 2004). However, for more realistic tropical-cyclone-like vortices that have an anticyclonic circulation in the upper troposphere, the interaction between the anticyclone aloft and cyclonic vortex below could cause a deflection of the surface track toward the left of the vertical shear vector (Wu and Emanuel, 1993; Wang and Holland, 1996c).

A fundamental question is how a TC vortex can sustain a coherent vertical structure in vertical shear. Wang and Holland (1996c) found in a numerical study that the cyclonic portion of the TC could remain upright in a moderate vertical shear. The TC core undergoes successive downshear tilting during the first 24-h while realigning over a 72-h period. A quasi-steady tilt to the downshear left was found even in the case where the diabatic heating was not considered. To understand the vertical alignment of a tilted TC vortex, Reasor and Montgomery (2001) developed a new theory, which separates the mean vortex evolution from the evolution of the tilt asymmetry. From this new perspective, the vertically-averaged azimuthal mean component of a tilted vortex is defined as the mean, while the departure from this mean as the tilt perturbation. The subsequent evolution of the tilt perturbation was captured by a linear, dry vortex Rossby wave (VRW) mechanism. They found that the continuum modes in the dynamical system destructively interact with the VRW, leading to the decay of the VRW and hence the vortex tilt. Schechter et al. (2002) viewed the vertical alignment as a result of the damping of the VRW due to its interaction with the mean vortex circulation. Reasor et al. (2004) show further that the VRW damping mechanism provides a direct means of eradicating the tilt of intense TC-like vortices in unidirectional vertical shear, and that intense TC-like vortices are much more resilient to vertical shear than previously believed. Therefore, the VRW damping mechanism intrinsic to the dry adiabatic dynamics of the TC vortex may play a crucial role in maintaining the vertically coherent structure of TCs in moderate vertical shear. However, how the diabatic heating including both the symmetric and asymmetric components affects this dry dynamics is still unknown and serves as an important topic of future study. Wong and Chan (2004) showed that the secondary circulation and the associated diabatic heating reduce the vertical tilt and the weakening of the TC, but the precise mechanisms remains to be addressed.

1.2.4. Spiral Bands

Along with the eye of the storm, spiral bands are one of the most recognized features of tropical cyclones. While the largest, “outer” bands have been easily seen on low-resolution satellite images for many years, increases in observational technology have led to the identification of spiral bands and “band-like” features on increasingly smaller scales, down to just a few hundred meters in size. These very small “streaks” are almost certainly a feature of the tropical cyclone boundary layer alone and are discussed above in section 1.2.2.2a; here, we will focus on bands with widths and separations distances of 4 km and larger, that extend through and above the depth of the boundary layer.

1.2.4.1 Ongoing studies of Inner-core bands

While not easily seen in satellite images, inner-core bands are clearly and almost universally observed in radar images of tropical cyclones ranging from strong tropical storm to category-5 intensity. These bands are typically 10-40 km in width, separated from each other on similar and larger scales, and show distinct spiral patterns radiating outward from the inner core (although they are not always “attached” to the eyewall).

Considerable effort from many different investigators has been put into establishing a dynamical mechanism for these bands. The most widely evaluated mechanism is the vortex-Rossby wave theory of Montgomery and Kallenbach (1997), which postulates that the bands of precipitation are associated with waves of PV which propagate radially and vertically on the PV gradient of the symmetric vortex. For low-wavenumber ($n=1$ to $n=2$) bands, substantial support for this theory has been presented since the last IWTC report. Careful analysis of high-resolution (3-6 km) numerical simulations of both real-case and idealized storms have shown a high spatial correlation between precipitation, clouds, and PV in the bands, strongly suggesting that the bands are coupled to vortex-Rossby waves (Chen and Yau 2001; Wang 2002a, b). These results were further supported by the “empirical normal mode” analysis of Chen et al. (2003), who found that 70-80% of the wave activity of the $n=1$ and $n=2$ bands could be dynamically represented by vortex-Rossby waves.

On the observational side, Reasor et al. (2000) found close correlation between $n=2$ bands of vorticity and reflectivity in pseudo-Dual-Doppler analyses of the inner core of Hurricane Olivia (1998). Very strong support for the predictions of vortex-Rossby wave theory in regards to the azimuthal and radial propagation of the bands was recently published by Corbosiero et al. (2006). They performed Fourier decompositions in the azimuthal direction of the radar features, relative to the centre of the storm. The $n=2$ components of the reflectivity were shown to propagate azimuthally (retrograding relative to the mean flow) and radially (outward) at speeds consistent with the phase and group speeds derived by Montgomery and Kallenbach (1997) and Moeller and Montgomery (2000).

For higher azimuthal wavenumbers ($n=3$ and higher), PV features, convection, and precipitation become less satisfyingly correlated, and vortex-Rossby wave theory is less successful in predicting their behaviour. This may be for several reasons. First, on smaller scales, the dynamics of the waves may be more heavily influenced by their coupling to convection; that is to say, the PV may be a “slave” to the precipitating band, rather than the other way around. Secondly, the inherent noisiness of a highly nonlinear fluid dynamical system with embedded nonlinear physical processes may make the correlations difficult to establish on smaller space and time scales. Finally, smaller-scale bands may have a different dynamical mechanism. This will now be discussed.

1.2.4.2 Smaller scale and “fine-scale” bands

In a widely cited paper, Gall et al. (1998) presented detailed analyses of land-based Doppler radar observations of Hugo (1989), Andrew (1992), and Erin (1995). Along with the inner core bands, they also found considerable evidence for numerous, even prolific bands on still smaller scales of 2-10 km, mostly within close range of the eyewall (Fig 1.2.7a). Unlike the larger inner-core bands, they found very little propagation of these smaller bands relative to the mean flow (even less than would be predicted by vortex-Rossby wave theory). They referred to these features as “fine-scale” spiral bands. Very recently, Kusunoki and Mashiko (2006) presented new observations of fine-scale bands, very similar to those of Gall et al. (1998), from radar observations of Typhoon Songda (2004) during its landfall at Okinawa.

In a high resolution (2 km) simulation of Hurricane Andrew, Yau et al. (2004) found fine-scale bands with horizontal scales and vertical structures very similar to those shown by Gall et al. (1998) (Fig 1.2.7b). The bands represented a high degree of, but not complete, correlation between PV, vertical velocity, precipitation, and low-level wind maxima. A budget analysis of the wind field showed that the wind streaks were caused by enhanced radial advection of the azimuthal wind field, in turn caused by enhanced vertical motion associated with latent heat release in the bands. However, an analysis of the propagation speed and evolution of these bands as compared to the predictions of vortex-Rossby wave theory was not presented in this study.

Nolan (2005) proposed that at least some of these features are not caused by radiating PV waves, but instead are convective bands triggered by large rolls in the hurricane boundary layer. His linearised,

global stability analysis of an unstratified swirling boundary layer, modelled after tropical cyclones, did find unstable modes in the form of streamwise rolls with similar scales to the fine-scale bands, that could spiral either inward, outward, or not at all (Fig 1.2.7d,e). The dynamics of these modes are essentially the same as the more common rolls in the Ekman-like planetary boundary layer, but with enhanced instability due to the much larger cross-stream component of the flow (the radial inflow and its reversal above the boundary layer). Foster (2005) treated the problem locally, allowing for stratification and more realistic wind profiles, and also found streamwise rolls (Fig 1.2.7f,g) on a wide range of scales, from those of the fine-scale bands to much smaller rolls embedded in the lowest levels of the boundary layer, as discussed in section 1.2.2.2.

In a further attempt to identify and understand the fine-scale bands, Romine and Wilhelmson (2006) analysed a very high resolution (1.1 km inner nest) simulation of Hurricane Opal (1995). The model reproduced the prolific small-scale bands in impressive detail (Fig 1.2.7c). Based on examination of the bands and larger flow field, Romine and Wilhelmson argue that the bands are a manifestation of Kelvin-Helmholtz instability associated with the strong low-level shear of the radial inflow, but modified by gravity wave dynamics and vertical variations of the stability parameter so as to acquire significant outward propagation. However, a more comprehensive analysis of the flow stability, as in Nolan (2005) or Foster (2005), or of the wave dynamics, as in Chen et al. (2003), will be required to validate this hypothesis.

1.2.4.3 Band features and dynamics associated with gravity waves

While some of the earliest theories of spiral bands attributed their existence to gravity waves embedded in a swirling flow (Diercks and Anthes 1976; Kurihara 1976; Willoughby 1978), such theories have not been supported by observations and simulations. The main disagreement is that spiral rainband features move quite slowly (or not at all) relative to the symmetric flow, while gravity waves propagate outward quite rapidly, with almost no interaction with the symmetric vortex (Nolan and Montgomery 2002).

Nonetheless, radiating gravity waves are endemic to tropical cyclone simulations, as shown by Chow et al. (2002). They are radiated from the eyewall and inner-core region by either isolated convective events or by convective asymmetries propagating on the eyewall, which themselves are often associated with trapped vortex-Rossby waves or even unstable modes. Chow et al. attribute the moving outer spiral rainbands to these waves, while Wang (2002a, b) showed that the outer rainbands (outside of about three times of the RMW) couldn't be explained by vortex-Rossby waves since the radial PV gradients become too weak to support them. Chow and Chan (2003) derived an Eliassen-Palm-Flux theory for radiating gravity waves in a shallow-water vortex, from which they estimated that gravity waves transport a large amount of angular momentum away from the core, as much as 10% per hour. However, this large loss of angular momentum cannot be reconciled with numerous other studies. Studies of the effects of asymmetric convection on tropical cyclones have found that virtually all of the dynamical effects are localized to the vicinity of the convective event, while any change to the wind field caused solely by the radiating gravity waves is insignificant in comparison (Nolan and Montgomery 2002; Nolan and Grasso 2003; Nolan et al. 2006).

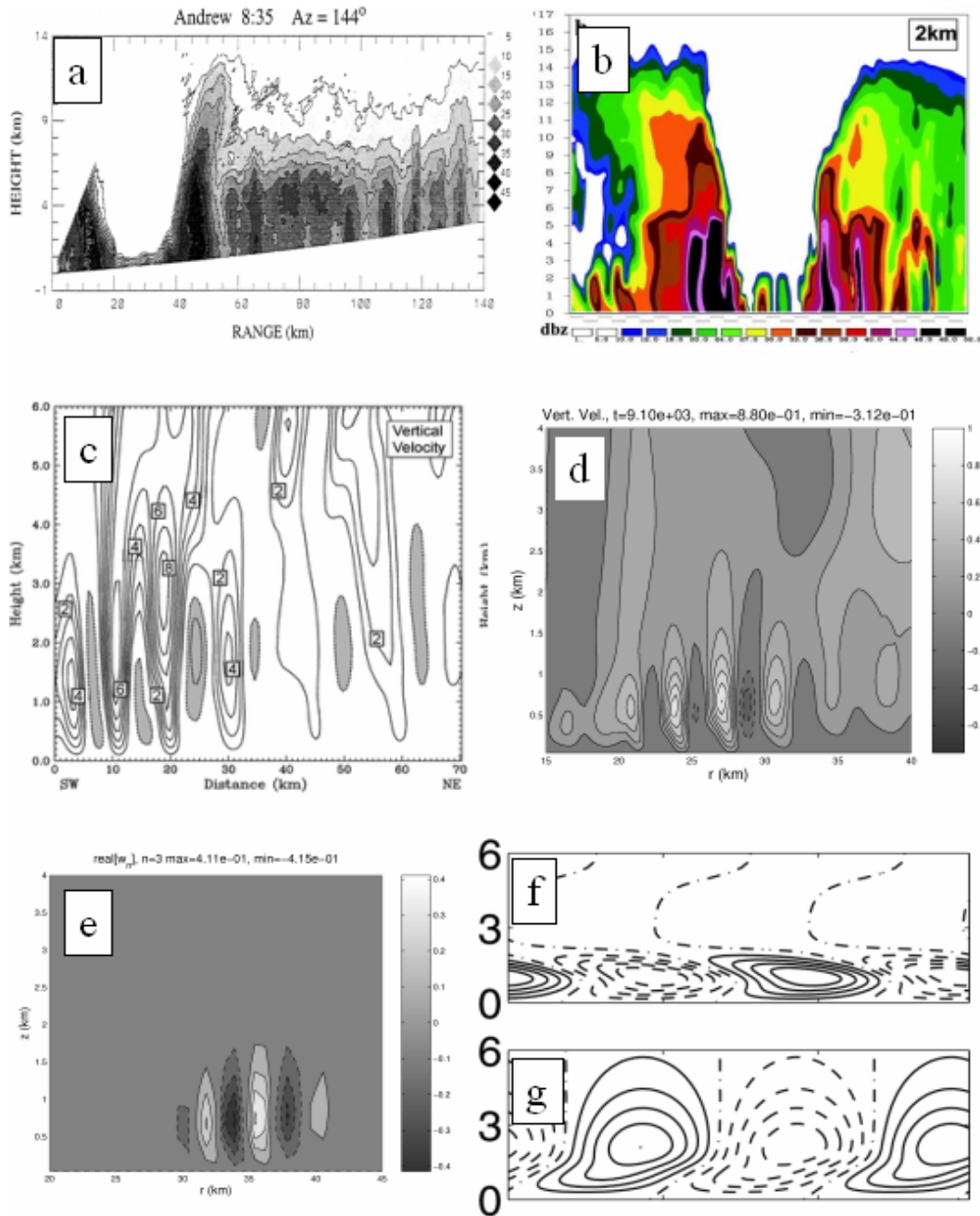


Figure 1.2.7: Observed, simulated, and predicted structures of fine-scale bands in various recent publications: a) radius-height radar cross-section of bands in Hurricane Andrew (1992) from Gall et al. (1998); b) radius-height cross-section of simulated reflectivity in a high-resolution simulation of Andrew from Yau et al. (2004); c) vertical motion in a vertical cross-section of a simulation of Hurricane Opal (1995) from Romine and Wilhelmson (2006); d) vertical motion as seen in highly idealized simulations on a hurricane-like boundary layer from Nolan (2005); e) analyzed structure of the global, most unstable mode of the same simulation as d; f) analyzed along-roll velocity of a local unstable mode in a more realistic boundary layer (with stratification) from Foster (2005); g) vertical velocity of the same mode as f.

1.2.4.4 RAINEX

In the Atlantic hurricane season of 2005, a very ambitious field project was undertaken by lead investigators from the University of Miami and the University of Washington, along with collaborators from NOAA/HRD, NCAR, and the U.S. Navy: the Rainband and Intensity Change Experiment (RAINEX). The goal of the project was the simultaneous observation of the eyewall, inner core, and inner core bands of mature tropical cyclones, with the purpose of trying to determine the role that rainbands play in tropical cyclone intensity changes. An ambitious aspect of the project was the use of three aircraft with on-board Doppler radars at the same time: the two NOAA P3 aircraft and the Navy P3 aircraft. Furthermore, real-time forecasts of the storms using an ensemble of mesoscale model runs (MM5 and WRF, run from various global model forecasts such as the GFS, NOGAPS, and CMC) were used to make daily decisions for flight operations.

Thanks in part to the amazingly high activity of the 2005 hurricane season, the observational phase of the project was an outstanding success. In particular, rainbands in the cores of mature hurricanes Katrina, Ophelia, and Rita were sampled extensively and repeatedly by multiple aircraft. In some cases, bands were observed from both sides at the same time, while in others, simultaneous eyewall evolution and rainband evolution were documented. Some noteworthy examples of observed features are the variation of the convective structure along the length of the bands, with convective cells preferred upwind/outward and stratiform precipitation preferred downwind/inward along the band, and detailed wind fields, vorticity, and secondary circulations in the vicinity of a developing secondary eyewall.

Analysis of the enormous reflectivity, Doppler wind, and dropsonde data sets from the RAINEX project have just begun. We expect that numerous publications will result between now and the next IWTC report.

1.2.4.5 Rainband activity and organization in regards to the TC environment

The organization of rainbands around the storm is known to be highly dependent on the surrounding environment. It is already well known that wind shear has a strong influence, with outer rainbands preferring the downshear right quadrant, often organizing into a single, long lasting "principal band" that leads the storm (Willoughby et al. 1984). Inner-core bands are also suppressed in the upshear quadrants. The organization of convective activity in regards to storm motion, vertical shear direction, and storm strength was documented by Lonfat et al. (2004) with composites of TRMM satellite rain rate observations from numerous storms around the world.

Two very recent studies have independently identified the size and strength of the "moisture envelope" around the storm as playing a significant role in organizing the bands. Using RAINEX and global satellite data to compare Hurricanes Katrina (2005) and Rita (2005), Ortt and Chen (2006) found that a large envelope of above average moisture around Katrina caused rainband formation over a very large area around the storm. A smaller moist envelope around Rita, however, suppressed the outer rainband activity, allowing for a more focused region of more intense inner core band activity in close vicinity of the storm. This in turn led to multiple eyewall replacement cycles for Rita, while only one such cycle occurred for Katrina as it traversed the gulf.

Similar changes in rainband organization were found by Kimball (2006) in mesoscale model simulations of the landfall of Hurricane Danny (1997). The specific humidity of the environment around the storm was modified with large and small-sized areas of enhanced and suppressed moisture. Larger and stronger moist envelopes led to enhanced rainband activity around the storm. The effects of these changes on storm intensity are discussed in the next section.

1.2.4.6 The effect of rainbands on hurricane intensity

Does the existence of spiral rainbands make hurricanes stronger, weaker, or have little effect? This is the over-arching question in hurricane research that focuses on spiral bands.

In past years spiral bands were seen as having a negative impact on intensity, as they steal some of the low level moist inflow into the eye of the storm, while simultaneously replacing that inflow with cooler, drier air from convective downdrafts (Barnes et al., 1983; Powell, 1990a, 1990b; Cione et al. 2000; Wang, 2002c; Wroe and Barnes, 2003). However, the introduction of cooler and drier air allows for more heat and moisture to be extracted from the ocean by the storm. Nonetheless, this extra heat and moisture simply replaces what is released in the rainbands, and latent heat release well away from the storm centre is believed to have very little effect on intensity (Hack and Schubert, 1986; Nolan et al., 2006).

From another thermodynamic point of view, however, rainbands may help maintain storm intensity in the face of shear and/or dry air associated with approaching troughs or jets. It is widely believed that “large” storms can resist the effects of shear and dry air for a longer time before the storm begins to weaken. This is in agreement with the simulations of Kimball (2006) described above. Kimball also observed that a “large-moist-envelope” storm with enhanced rainband activity intensified more slowly. Thus, the thermodynamic effect of rainbands on a tropical cyclone likely depends on the stage of development of the storm.

There is ongoing research about the effects of rainbands on cyclone intensity from a fluid dynamical point of view. Spiral bands of convection seem to both be caused by, and to generate, spiral bands of PV. These spiral features are examples of vorticity perturbations that are tilted “downshear” in a stable, sheared flow. Such perturbations are universally associated with an “upgradient” (in this case, inward) transport of angular momentum, leading to a small increase in the intensity of the storm (Carr and Williams 1989; Montgomery and Kallenbach 1997; Nolan and Farrell 1999b; Moeller and Montgomery 1999, 2000; May and Holland 1999; Chen et al. 2003). However, recent results by Nolan and Grasso (2003) and Nolan et al. (2006) suggest this conclusion may be incomplete. By simulating the generation of vortex-Rossby waves from isolated convective events embedded in a vortex, they found that while the waves themselves cause an intensifying effect on the vortex, the adjustment process whereby the bands were created had an even larger negative effect. In any case, the net effect of the “asymmetric” dynamics was trivial compared to the effect of the azimuthally averaged heating. Thus, while spiral rainbands may be associated with inward transport of angular momentum and vorticity, their net effect on the storm is more likely dominated by the azimuthally averaged secondary circulation generated by their associated convection and latent heat release.

As before, then, the overall impact of spiral rainbands on tropical cyclone intensity cannot be stated in generalities. Recent advances, however, are leading to a broader understanding from which the effects of rainbands can be inferred on a case-by-case basis.

1.2.5. Implications for Forecasting

Our ability to accurately forecast hurricane motion (track) has improved dramatically in the past 20 years, largely because of the improving ability to capture evolving synoptic-scale fields with present numerical guidance. The track is controlled almost entirely by the environmental steering flow in which the storm vortex is embedded, and which is increasingly well depicted in global- and regional-scale NWP. In contrast, our ability to forecast hurricane intensity change has shown quite limited progress in the past 20 years and again it is widely believed that this is due to our present inability to model small-scale internal processes in hurricanes. Here, we discuss the implications of the recent gains in our knowledge of inner-core structure and dynamics, as reviewed in previous sections, on the

forecasting of intensity and track.

1.2.5.1 Inner core influences on forecasting intensity and intensity change

Intensity, when measured in terms of near-surface wind speed, is determined partly by the properties of the boundary layer. The boundary layer has been shown by theory, models and observations to be very inhomogeneous, particularly in the vicinity of the eyewall. The most direct impact of this for intensity estimation and forecasting is that the surface wind factor is higher beneath the eyewall than at larger radius (0.9 instead of 0.8), and is frequently higher on the weak (left in the Northern Hemisphere) side of the storm.

Measurements of near-surface turbulence have tended to confirm existing gust factors. Strong evidence for boundary layer rolls explains the observed streakiness of damage in some storms, and may indicate higher risk than has hitherto been supposed.

The eyewall replacement cycle has been known for decades, but satellite microwave observations continue to improve our ability to monitor it, and to make short-term predictions by extrapolation. Such ability is particularly high at the moment, due to the large number of satellites in operations, and unlikely to be sustained.

Mesoscale vortices on the inner edge of the eyewall have been shown to be associated with locally enhanced winds. They thus present an additional hazard, as well as playing a key role in cyclone dynamics. While observations have generally been in very vertical storms, there is some evidence that they also occur in tilted systems. Their hypothesised role in the formation of “annular hurricanes” is significant to forecasting, since such storms have been shown to decay at significantly less than the climatological rate. Moreover, the fact that they can cause significant rearrangements of the inner core structure, including weaker winds with lower central pressure, casts doubt on the long-established practice of regarding maximum wind and central pressure as quasi-equivalent measures of storm intensity.

Rainbands continue to have an uncertain impact on TC intensity: they consume some of the energy-rich low-level moist inflow, but may protect the inner core from environmental shear, and also produce intensification through the transport of angular momentum into the storm centre.

Numerical weather prediction (NWP) of these changes remains challenging. Many of the relevant features are short-lived and evolve rapidly. Their initiation may depend on small-scale, poorly-observed features in the storm. The dynamics may be so different to much of the rest of the atmosphere, and the physics of the observations so complicated (e.g. ice scattering in passive microwave satellite imagery) that data assimilation systems are stretched to interpret it. The time-scale may also be much less than the traditional 6-hourly NWP cycle. Nevertheless, a few encouraging preliminary results have been achieved.

Intensity change is also strongly influenced by external forcing, either from the atmospheric environment surrounding the storm, from the ocean, or from nearby land and orography. These are covered in detail in subtopics 1.1 and 1.3. Subtopic 1.5 focuses directly on the operational forecasting of structure change.

1.2.5.2 Inner core influences on forecasting track

In contrast to intensity, the influence of the inner core on forecasting track is modest. Small-scale asymmetries can give rise to a trochoidal oscillation (e.g. Muramatsu, 1986; Nolan et al., 2001), but the small amplitude relative to the scale of the storm, and short time-scale of the oscillation relative to operational cycles, means that this will have only slight operational significance.

1.2.6. Conclusions

Better observations and theoretical advances have resulted in significant improvements in understanding. A short summary of the highlights follows:

- There have been significant advances in knowledge and understanding of surface winds on several scales: the mean, coherent boundary-layer structures, and turbulence.
- The winds in the upper boundary-layer are supergradient in some storms.
- Multiple satellites and radars are providing an unprecedented view of the eyewall replacement cycle, shedding new light on its occurrence and importance in storm dynamics. These observations are informing operational forecasts of intensity change, on occasion.
- Eyewall mesovortices provide an added hazard in some storms, and play an important role in storm dynamics and intensity change.
- Vortex Rossby waves explain observations of inner-core spiral bands, and play an important role in the storm dynamics, including in genesis, resistance to shear, and intensification. Fine-scale bands may be from other causes, including boundary layer instabilities.

1.2.7. Recommendations for Research and Operations

Boundary layer winds. How much of the inter- and intra-storm variability in surface wind factor is predictable? How does this compare with other sources of uncertainty in intensity estimation? How important is stability? What are suitable gust factors over the sea/land/beneath the eyewall/at larger radius? Is it necessary/possible to predict the occurrence/intensity of rolls?

Wind-field expansion. This is clearly operationally important (e.g. H. Katrina's surge) but little (nothing?) is known of the dynamics. How well can we predict this?

Eyewall mesovortices. How prevalent are these? In vertical/tilted storms? How often are they sufficiently intense to represent a significant additional hazard? Can their formation be predicted (for application to intensity change, annular hurricanes)?

Spiral bands. In the inner core, vortex Rossby waves are an important, but not the sole, influence. But at larger radius? What is the role of gravity waves? And the implication for numerical modelling? Do the wind perturbations associated with fine-scale inner bands matter for risk estimation? Do spiral bands intensify or weaken the storm, or does it depend on the situation? If so, how?

Numerical Weather Prediction. Which of these small-scale features can be predicted? How far ahead? What are the issues for assimilation of various data types in tropical cyclones? Do assimilation systems contain the right balances for tropical cyclones?

Empirical Prediction. How can knowledge of these processes improve forecasts? Especially in the last few hours before landfall when they may be visible on radar as well as satellite? Can Doppler radar algorithms (e.g. EVTD) be used in real-time? How can these be shared around the world? How will emergency services respond to such "last-minute" information? What are the limits on intensification/decay rates? What are the precursors of intensification/decay on various types of satellite imagery? How close must land/islands be before they start to affect structure?

Acronyms

AMSR-E	Advanced Scanning Microwave Radiometer for EOS
BL	Boundary-layer
EMV	Eyewall mesovortex
ERC	Eyewall replacement cycle
EVTD	Extended Velocity Track Display
IR	Infrared
MHS-1	Microwave Humidity Sounder
NHC	National Hurricane Center
NRC	National Research Council
PI	Potential intensity
PV	Potential vorticity
RMW	Radius of maximum (tangential?) wind speed
SFMR	Stepped-frequency microwave radiometer
SSM/I	Special Sensor Microwave Imager
SSMIS	Special Sensor Microwave Imager/Sounder
SST	Sea surface temperature
SWF	Surface wind factor
TC	Tropical cyclone
TCBL	Tropical cyclone boundary layer
TMI	TRMM Microwave Imager
TRMM	Tropical Rainfall Measuring Mission

Bibliography

Note that most, but not all these references are cited in the text - the bibliography is intended to be as exhaustive as we could make it.

Aberson, S.D. and J.B. Halverson. 2006: Kelvin–Helmholtz billows in the eyewall of Hurricane Erin. *Mon. Wea. Rev.*, **134**, 1036–1038.

Aberson, S.D., J.P. Dunion and F.D. Marks Jr., 2006: A photograph of a wavenumber-2 asymmetry in the eye of Hurricane Erin. *J. Atmos. Sci.*, **63**, 387–391.

Aberson, S.D. and D.P. Stern, 2006: Extreme horizontal winds measured by dropwindsondes in hurricanes. *Extended Abstracts, 27th Conference on Hurricanes and Tropical Meteorology*, Amer. Meteor. Soc., Monterey, Ca, 24 - 28 April. CD-ROM.

Barnes, G.M., E.J. Zipser, D.P. Jorgensen and F.D. Marks Jr., 1983: Mesoscale and convective structure of a hurricane rainband. *J. Atmos. Sci.*, **40**, 2125-2137.

Bender, M.A., 1997: The effect of relative flow on the asymmetric structure in the interior of hurricanes. *J. Atmos. Sci.*, **54**, 703 - 724.

Bister, M., 2001: Effect of Peripheral Convection on Tropical Cyclone Formation. *J. Atmos. Sci.* **58**, 3463-3476.

Black, M.L.; Gamache, J.F.; Marks, F.D. Jr; Samsury, C.E.; Willoughby, H.E., 2002: Eastern Pacific Hurricanes Jimena of 1991 and Olivia of 1994: The Effect of Vertical Shear on Structure and Intensity. *Mon. Weather Rev.* **130**, 2291-2312

- Black, P. G., and F. D. Marks, 1991: The structure of an eyewall meso-vortex in Hurricane Hugo (1989). Preprints, *19th Conf. on Hurricanes and Tropical Meteorology*, Miami, FL, Amer. Meteor. Soc., 579–582.
- Braun, S.A., 2002: A Cloud-Resolving Simulation of Hurricane Bob (1991): Storm Structure and Eyewall Buoyancy. *Mon. Wea. Rev.*, **130**, 1573-1592.
- Braun, S.A., M.T. Montgomery and Z. Pu. 2006: High-Resolution Simulation of Hurricane Bonnie (1998). Part I: The organization of eyewall vertical motion. *J. Atmos. Sci.*, **63**, 19–42.
- Brown, R. A., and L. Zeng, 2001: Comparison of Planetary Boundary Layer Model Winds with Dropsonde Observations in Tropical Cyclones. *J. AMeteor.*, **40**, 1718-1723.
- Camp, J. P., and M. T. Montgomery, 2001: Hurricane Maximum Intensity: Past and Present. *Mon. Wea. Rev.*, **129**, 1704-1717.
- Cangialosi, J.P., S.S. Chen, W. Zhao, W. Wang, and J. Michalakis, 2006: Real-time high-resolution MM5 and WRF forecasts during RAINEX. *Extended Abstracts, 27th Conference on Hurricanes and Tropical Meteorology*, Amer. Meteor. Soc., Monterey, Ca, 24 - 28 April. CD-ROM.
- Carr, L.E. III and R.T. Williams. 1989: Barotropic Vortex Stability to Perturbations from Axisymmetry. *J. Atmos. Sci.*, **46**, 3177–3191.
- Cervený, Randall S.; Balling, Robert C. 2005: Variations in the Diurnal Character of Tropical Cyclone Wind Speeds. *Geophys. Res. Lett.*: **32**, L06706.
- Chen, Y., and M. K. Yau, 2001: Spiral Bands in a Simulated Hurricane. Part I: Vortex Rossby Wave Verification. *J. Atmos. Sci.*, **58**, 2128-2145.
- Chen, Y., G. Brunet, and M. K. Yau. 2003: Spiral Bands in a Simulated Hurricane. Part II: Wave Activity Diagnostics. *J. Atmos. Sci.*. **60**, 1239-1256.
- Chow, K. C., Chan, K. L., Lau, A.K.H.. 2002: Generation of Moving Spiral Bands in Tropical Cyclones. *J. Atmos. Sci.*. **59**, 2930–2950.
- Chow, K.C. and K.L. Chan, 2003: Angular momentum transports by moving spiral waves. *J. Atmos. Sci.*, **60**, 2004-2009.
- Cione, J.J., P.G. Black and S.H. Houston, 2000: Surface wind observations in the hurricane environment. *Mon. Wea. Rev.*, **128**, 1550-1561.
- Corbosiero, K., and J. Molinari, 2002: The effects of vertical wind shear on the distribution of convection in tropical cyclones. *Mon. Wea. Rev.*, **130**, 2110-2123.
- Corbosiero, K., and J. Molinari, 2003: The relationship between storm motion, vertical wind shear, and convective asymmetries in tropical cyclones. *J. Atmos. Sci.*, **60**, 366-376.
- Corbosiero, Kristen L., John Molinari and Michael L. Black. 2005: The Structure and Evolution of Hurricane Elena (1985). Part I: Symmetric Intensification. *Mon. Wea. Rev.*: **133**, 2905–2921
- Corbosiero, K. L., J. Molinari, and A. R. Aiyyer, 2006: The structure and evolution of Hurricane Elena (1985). Part II: Convective asymmetries and evidence for vortex-Rossby waves. *Mon. Wea. Rev.*, in press.
- Cram, T. A., J. A. Knaff, M. DeMaria, and J. P. Kossin, 2006, Objective identification of annular

- hurricanes using GOES and reanalysis data, *AMS 27th Conf. on Hurricanes and Tropical Meteorology*, CD-ROM.
- Croxford, M., and G. M. Barnes, 2002: Inner core strength of Atlantic tropical cyclones. *Mon. Wea. Rev.*, **130**, 127-139.
- Dengler K., and D. Keyser (2000) Intensification of tropical cyclone-like vortices in uniform zonal background flows. *Quart. J. Roy. Meteor. Soc.*, **126**, 549–568.
- Diercks, J.W. and R.A. Anthes. 1976: A Study of Spiral Bands in a Linear Model of a Cyclonic Vortex. *J. Atmos. Sci.*, **33**, 1714–1729.
- Dunion, J.P., C.W. Landsea, S.H. Houston, And M.D. Powell, 2003: A Reanalysis of the Surface Winds for Hurricane Donna of 1960, *Mon. Wea. Rev.*, **131**, 1992-2011.
- Eastin, M.D., 2002. Observational analysis of buoyancy in intense hurricane eyewalls. *Extended abstracts, 24th Conference on Hurricanes and Tropical Meteorology*, American Meteorological Society, Boston, pp. 640–641.
- Eastin, M.D., 2003. *Buoyancy of convective vertical motions in the inner core of intense hurricanes*. Ph.D. dissertation, Department of Atmospheric Science, Colorado State University, Fort Collins, Colorado 80521, USA, p. 152.
- Eastin, M.D., W.M. Gray and P.G. Black. 2005a: Buoyancy of Convective Vertical Motions in the Inner Core of Intense Hurricanes. Part I: General Statistics. *Mon. Wea. Rev.*: **133**, 188–208
- Eastin, M.D., W.M. Gray and P.G. Black. 2005b: Buoyancy of Convective Vertical Motions in the Inner Core of Intense Hurricanes. Part II: Case Studies. *Mon. Wea. Rev.*: **133**, 209–227
- Eliassen, A. and M. Lystad, 1977: The Ekman layer of a circular vortex: A numerical and theoretical study. *Geophysica Norvegica*, **31**, 1-16.
- Emanuel, K.A., 1986: An air-sea interaction theory for tropical cyclones. Part I: Steady-state maintenance. *J. Atmos. Sci.*, **43**, 585-604.
- Emanuel, K.A., 1991: The theory of hurricanes. *Ann. Rev. Fluid Mech.*, **23**, 179-196.
- Emanuel, K.A., 1995: Sensitivity of tropical cyclones to surface exchange coefficients and a revised steady-state model incorporating eye dynamics. *J. Atmos. Sci.*, **52**, 3969-3976.
- Emanuel, K.A., 2000: A statistical analysis of tropical cyclone intensity. *Mon. Wea. Rev.*, **128**, 1139 - 1152.
- Emanuel, Kerry, C. DesAutels, C. Holloway and R. Korty. 2004: Environmental Control of Tropical Cyclone Intensity. *J. Atmos. Sci.*, **61**, 843-858.
- Etling, D., and R.A. Brown, 1993: Roll vortices in the planetary boundary layer: A review. *Boundary Layer Meteorology*, **65**, 215-248.
- Evans, J.L. and R. Hart, 2003: Objective indicators of the extratropical transition lifecycle of Atlantic tropical cyclones. *Mon. Wea. Rev.*, **131**, 909-925.
- Farfán, L. M., and J. A. Zehnder, 2001: An Analysis of the Landfall of Hurricane Nora (1997). *Mon. Wea. Rev.*, **129**, 2073-2088.

- Foster, R.C., 2005: Why Rolls are Prevalent in the Hurricane Boundary Layer. *J. Atmos. Sci.*: **62**, 2647–2661
- Frank, W.M., and E.A. Ritchie, 1999: Effects of environmental flow upon tropical cyclone structure. *Mon. Wea. Rev.*, **127**, 2044-2061.
- Frank, W. M., and E. A. Ritchie, 2001: Effects of Vertical Wind Shear on the Intensity and Structure of Numerically Simulated Hurricanes. *Mon. Wea. Rev.*, **129**, 2249-2269.
- Franklin, J.L., M.L. Black and K. Valde, 2003: GPS dropwindsonde wind profiles in hurricanes and their operational implications. *Wea. and Forecasting*, **18**, 32-44.
- Free, Melissa, M. Bister and K. Emanuel. 2004: Potential Intensity of Tropical Cyclones: Comparison of Results from Radiosonde and Reanalysis Data. *Journal of Climate*: **17**, 1722-1727.
- Gall, R., J. Tuttle, and P. Hildebrand, 1998: Small-scale spiral bands observed in hurricanes Andrew, Hugo, and Erin. *Mon. Wea. Rev.*, **126**, 1749-1766.
- Hack, J.J. and W.H. Schubert. 1986: Nonlinear Response of Atmospheric Vortices to Heating by Organized Cumulus Convection. *J. Atmo. Sci.*, **43**, 1559–1573.
- Halverson, J. B., J. Simpson, G. Heymsfield, H. Pierce, T. Hock and L. Ritchie. 2006: Warm core structure of Hurricane Erin diagnosed from high altitude dropsondes during CAMEX-4. *J. Atmos. Sci.*, **63**, 309–324.
- Hanley, D., J. Molinari and D. Keyser. 2001: A Composite Study of the Interactions between Tropical Cyclones and Upper-Tropospheric Troughs. *Mon. Wea. Rev.*, **129**, 2570–2584.
- Hart, R., 2003: A cyclone phase space derived from thermal wind and thermal asymmetry. *Mon. Wea. Rev.*, **131**, 585-616.
- Hausman, S.A., K.V. Ooyama and W.H. Schubert. 2006: Potential vorticity structure of simulated hurricanes. *J. Atmos. Sci.*, **63**, 87–108.
- Hawkins, J. D., T. F. Lee, K. Richardson, C. Sampson, F. J. Turk, and J. E. Kent, 2001, Satellite multi-sensor tropical cyclone structure monitoring, *Bull. Amer. Meteor. Soc.*, **82**, 567-578.
- Hawkins, J. D., and M. Helveston, 2004, Tropical cyclone multi-eyewall characteristics, *Preprints AMS 26th Hurricane and Tropical Meteorology Conference*, 276-277.
- Hawkins, J. D., M. Helveston, T. F. Lee, F. J. Turk, K. Richardson, C. Sampson, J. Kent and R. Wade, 2006, Tropical cyclone multiple eyewall configurations, *27th AMS Conference on Hurricanes and Tropical Meteorology*, CD-ROM.
- Hendricks, E.A.; Montgomery, M.T.; Davis, C.A., 2004: The Role of 'Vortical' Hot Towers in the Formation of Tropical Cyclone Diana (1984). *J. Atmos. Sci.* **61**, 1209-1232.
- Henning, R.G. , 2006: The intensity of wind gust underneath areas of deep eyewall convection in Hurricanes Katrina and Dennis at landfall. *Extended Abstracts, 27th Conference on Hurricanes and Tropical Meteorology*, Amer. Meteor. Soc., Monterey, Ca, 24 - 28 April. CD-ROM.
- Heymsfield, G. M., J. B. Halverson, J. Simpson, L. Tian, and T. P. Bui, 2001: ER-2 Doppler Radar Investigations of the Eyewall of Hurricane Bonnie during the Convection and Moisture Experiment-3. *J. AMeteor.*, **40**, 1310-1330.

- Heymnsfield, G.M., Halverson, J, Ritchie, E.A., Simpson, J, Molinari, J., Tian, L., 2006: Structure of highly sheared Tropical Storm Chantal during CAMEX-4. *J. Atmos. Sci.* 63, 268-287.
- Hock, T.F. and J.L. Franklin, 1999: The NCAR GPS dropwindsonde. *Bull. Amer. Meteor. Soc.*, **80**, 407-420.
- Holland, G.J., 1980: An analytic model of the wind and pressure profiles in hurricanes. *Mon. Wea. Rev.*, **108**, 1212-1218.
- Holland, G.J. and R.T. Merrill, 1984: On the dynamics of tropical cyclone structural changes. *Quart. J. Roy. Meteorol. Soc.*, **110**, 723-745.
- Holland, G.J, and M.Lander, 1993: The meandering nature of tropical cyclone tracks. *J. Atmos. Sci.*, **50**, 1254-1266.
- Hollinger, J., 1989, *DMSP Special Sensor Microwave/Imager calibration /validation. Final Rep. Vol. 1*. Naval Research Laboratory, 153 pp. [Available from the Naval Research Laboratory, Washington, DC, 20375].
- Horstmann, J.; Thompson, D.R.; Monaldo, F.; Iris, S.; Graber, H.C. 2005: Can Synthetic Aperture Radars be Used to Estimate Hurricane Force Winds? *Geophys. Res. Lett.*: **32**, L22801
- Hoskins, B.J., M.E. McIntye, and A.W. Robertson, 1985: On the use and significance of isentropic potential vorticity maps. *Q. J. Roy. Meteor. Soc.*, **121**, 821-851.
- Jones, S.C., 1995: The evolution of vortices in vertical shear. Part I: Initially barotropic vortices. *Quart. J. Roy. Meteorol. Soc.*, **121**, 821 - 851.
- Jones S.C., 2000: The evolution of vortices in vertical shear. II: Large-scale asymmetries. *Quart. J. Roy. Meteor. Soc.*, 3137-3160.
- Jones S.C., 2000: The evolution of vortices in vertical shear. III: Baroclinic vortices. *Quart. J. Roy. Meteor. Soc.*, 3161-3186.
- Jones, Sarah C. 2004: On the Ability of Dry Tropical-Cyclone-like Vortices to Withstand Vertical Shear. *J. Atmos. Sci.*: **61**, 114-119.
- Kaplan, John, DeMaria, Mark. 2003: Large-Scale Characteristics of Rapidly Intensifying Tropical Cyclones in the North Atlantic Basin. *Weather and Forecasting*. **18**, 1093–1108.
- Katsaros, K. B., P. W. Vachon, W. T. Liu, and P. G. Black, 2002: Microwave remote sensing of tropical cyclones from space. *J. Oceanogr.*, **58**, 137–151.
- Kelley, Owen A.; Stout, John; Halverson, Jeffrey B. 2005: Hurricane Intensification Detected by Continuously Monitoring Precipitation in the Eyewall. *Geophys. Res. Lett.*: **32**, L20819.
- Keper, J. D., 2001: The Dynamics of boundary layer jets within the tropical cyclone core. Part I : Linear Theory *J. Atmos. Sci.*, **58**, 2469-2484.
- Keper, J. D. and Y. Wang, 2001: The Dynamics of boundary layer jets within the tropical cyclone core. Part II : Nonlinear enhancement *J. Atmos. Sci.*, **58**, 2485-2501.
- Keper, J.D., 2002a: The impact of landfall on tropical cyclone boundary layer winds. *Extended*

- abstracts, 25th Conference on Hurricanes and Tropical Meteorology, Amer. Meteor. Soc., San Diego, California, 29 April - 3 May, 2002, 335-336.
- Kepert, J.D., 2002b: Modelling the tropical cyclone boundary layer wind-field at landfall. *Extended abstracts, 14th BMRC Modelling Workshop: Modelling and Predicting Extreme Events*, Melbourne, Australia, 11-13 November, 81-84.
- Kepert, J.D., 2002c: *The Wind-Field Structure of the Tropical Cyclone Boundary-Layer*. PhD thesis, Monash University, Melbourne, Australia. 350 pp.
- Kepert, J.D. 2004: Models and observations of tropical cyclone boundary-layer winds. *BMRC Research Report No 104: The Past, Present and Future of Numerical Modelling: extended abstracts of presentations at the sixteenth annual BMRC Modelling Workshop 6-9 December 2004*. Melbourne, Australia. pp 77-82.
- Kepert, Jeffrey D., 2005: Objective Analysis of Tropical Cyclone Location and Motion from High-Density Observations. *Mon. Wea. Rev.*: **133**, 2406–2421.
- Kepert, J.D., 2006a: Observed boundary-layer wind structure and balance in the hurricane core. Part I: Hurricane Georges. In press, *J. Atmos. Sci.*
- Kepert, J.D., 2006b: Observed boundary-layer wind structure and balance in the hurricane core. Part II: Hurricane Mitch. In press *J. Atmos. Sci.*
- Kim, S.Y.; Chun, H.Y.; Baik, J.J. 2005: A Numerical Study of Gravity Waves Induced by Convection Associated with Typhoon Rusa. *Geophys. Res. Lett.*: **32**, L24816.
- Kimball, S.K., 2006: A modelling study of hurricane landfall in a dry environment. *Mon. Wea. Rev.*, **134**, 1901-1918.
- Kishtawal, C.M.; Patadia, Falguni; Singh, Randhir, Basu, Sujit; Narayanan, M.S.; Joshi, P.C. 2005: Automatic Estimation of tropical Cyclone Intensity Using Multi-Channel TMI Data: A genetic Algorithm Approach. *Geophys. Res. Lett.*: **32**, L11804.
- Knaff, J. A., J. P. Kossin, and M. DeMaria, 2003, Annular hurricanes, *Wea. & Forecasting*, **18**, 204-223.
- Knaff, John A., S. A. Seseske, M. DeMaria and J. L. Demuth. 2004: On the Influences of Vertical Wind Shear on Symmetric Tropical Cyclone Structure Derived from AMSU. *Mon. Wea. Rev.*: **132**, 2503-2510.
- Knupp, K.R., J. Walters, and E.W. McCaul Jr, 2000: Doppler profiler observations of Hurricane Georges at landfall. *Geophysical Research Letters*, **27**, 3361-3364.
- Knupp K.R., J. Walters, M. Biggerstaff, 2005: Doppler Profiler and Radar Observations of Boundary Layer Variability during the Landfall of Tropical Storm Gabrielle. *J. Atmos. Sci.*, **63**, 234-251.
- Kodama, Yasu-Masa and Takuya Yamada. 2005: Detectability and Configuration of Tropical Cyclone Eyes over the Western North Pacific in TRMM PR and IR Observations. *Mon. Wea. Rev.*: **133**, 2213–2226
- Kodama, Y., T. Yamada, 2005, Detectability and configuration of tropical cyclone eyes over the western north Pacific in TRMM PR and IR observations, *Mon. Wea. Rev.*, **133**, 2213-2226.
- Kossin, J. P., Schubert W. T., Montgomery M. T., 2000: Unstable interactions between a hurricane's

- primary eyewall and a secondary ring of enhanced vorticity. *J. Atmos. Sci.* **57**, 3893-3917.
- Kossin, J. P., and M. D. Eastin, 2001: Two Distinct Regimes in the Kinematic and Thermodynamic Structure of the Hurricane Eye and Eyewall. *J. Atmos. Sci.*, **58**, 1079-1090.
- Kossin, J. P., and W. H. Schubert, 2001: Mesovortices, Polygonal Flow Patterns, and Rapid Pressure Falls in Hurricane-Like Vortices. *J. Atmos. Sci.*, **58**, 2196-2209.
- Kossin, J. P., B. D. McNoldy, and W. H. Schubert, 2002: Vortical swirls in hurricane eye clouds. *Mon. Wea. Rev.*, **130**, 3144-3149
- Kossin, J. P., and W. H. Schubert, 2003: Diffusion versus advective rearrangement of a circular vortex sheet. *J. Atmos. Sci.* **60**, 586-589.
- Kossin, J., H. Berger, J. Hawkins, and T. Cram, 2006: Development of a secondary eyewall formation index for improvement of tropical cyclone intensity forecasting. *Proceedings, 60th Interdepartmental Hurricane Conference (IHC), Mobile, AL.*
- Kossin, J. P. and Wayne H. Schubert 2005: Mesovortices in Hurricane Isabel. *Bull. Amer. Meteorol. Soc.*: **85**, 151-153.
- Krishnamurti, T. N., S. Pattnaik, L. Stefanova, T. S. V. Vijaya Kumar, B. P. Mackey, A. J. O'Shay and Richard J. Pasch. 2005: The Hurricane Intensity Issue. *Mon. Wea. Rev.*: **133**, 1886-1912
- Kuo, H.-C., R. T. Williams and J.-H. Chen. 1999: A Possible Mechanism for the Eye Rotation of Typhoon Herb. *J. Atmos. Sci.*, **56**, 1659-1673.
- Kuo, H.-C., L.-Y. Lin, C.-P. Chang and R. T. Williams. 2004: The Formation of Concentric Vorticity Structures in Typhoons. *J. Atmos. Sci.*: **61**, 2722-2734.
- Kuo, H.L., 1971: Axisymmetric flow in the boundary layer of a maintained vortex. *J. Atmos. Sci.*, **28**, 20-41.
- Kuo, H.L., 1982: Vortex boundary layer under quadratic surface stress. *Boundary-Layer Meteorol.*, **22**, 151-169.
- Kurihara, Y., 1976: On the development of spiral bands in a tropical cyclone. *J. Atmos. Sci.*, **33**, 940-958.
- Kurihara, Y.; Bender, M.A.; Ross, R.J., 1993: An initialization scheme of hurricane models by vortex specification. *Mon. Wea. Rev.*, **121**, 2030-2045.
- Kurihara, Y.; Bender, M.A; Tuleya, R.E.; Ross, R.J., 1995: Improvements in the GFDL hurricane prediction system. *Mon. Wea. Rev.*, **123**, 2791-2801.
- Kusunoki, K., 2006: Assessment of the Doppler radar for airport weather (draw) system in Japan as a research tool for studying typhoon. *Extended Abstracts, 27th Conference on Hurricanes and Tropical Meteorology*, Amer. Meteor. Soc., Monterey, Ca, 24 - 28 April. CD-ROM.
- Kusunoki, K. and W. Mashiko, 2006: Doppler radar investigations of the inner core of typhoon songda (2004): polygonal/ elliptical eyewalls, eye contraction, and small-scale spiral bands. *Extended Abstracts, 27th Conference on Hurricanes and Tropical Meteorology*, Amer. Meteor. Soc., Monterey, Ca, 24 - 28 April. CD-ROM.
- Kwok J.H.Y. and J. C. L. Chan. 2005: The Influence of Uniform Flow on Tropical Cyclone Intensity

Change. *J. Atmos. Sci.*: **62**, 3193–3212

Kwon Y.C. and W.M. Frank. 2005: Dynamic Instabilities of Simulated Hurricane-like Vortices and Their Impacts on the Core Structure of Hurricanes. Part I: Dry Experiments. *J. Atmos. Sci.*: **62**, 3955–3973.

Lackmann, Gary M. and R. M. Yablonsky. 2004: The Importance of the Precipitation Mass Sink in Tropical Cyclones and Other Heavily Precipitating Systems. *J. Atmos. Sci.*: **61**, 1674-1692.

Landsea, Christopher W., J. L. Franklin, C. J. McAdie, J. L. Beven II, J. M. Gross, B. R. Jarvinen, R. J. Pasch, E. N. Rappaport, J. P. Dunion and P. P. Dodge. 2004: A Reanalysis of Hurricane Andrew's Intensity. *Bull. Amer. Meteorol. Soc.*: **85**, 1699-1712.

Lee, W.-C., B. J.-D. Jou, P. L. Chang, and S.-M. Deng, 1999: Tropical cyclone kinematic structure retrieved from single Doppler radar observations. Part I: Interpretation of Doppler velocity patterns and the GBVTD technique. *Mon. Wea. Rev.*, **127**, 2419-2439.

Lee, W.-C., and F. D. Marks Jr., 2000: Tropical cyclone kinematic structure retrieved from single Doppler radar observations. Part II: The GBVTD-simplex center finding algorithm. *Mon. Wea. Rev.*, **128**, 1925-1936.

Lee, W.-C., B. J.-D. Jou, P. L. Chang, and F. D. Marks Jr., 2000: Tropical cyclone kinematic structure retrieved from single Doppler radar observations. Part III: Evolution and structure of Typhoon Alex (1987). *Mon. Wea. Rev.*, **128**, 3982-4001.

Lee, T. F., F. J. Turk, J. D. Hawkins, and K. A. Richardson, 2002, Interpretation of TRMM TMI images of tropical cyclones, *Earth Interactions E-Journal*, **6**, 3.

Lewis, B.M. and H.F., Hawkins, 1982: Polygonal eye walls and rainbands in hurricanes. *Bull. Amer. Meteor. Soc.*, **63**, 1294-1301.

Liang, Xudong and Johnny C. L. Chan. 2005: The Effects of the Full Coriolis Force on the Structure and Motion of a Tropical Cyclone. Part I: Effects due to Vertical Motion. *J. Atmos. Sci.*: **62**, 3825–3830.

Lin, Y.-L., D.B. Ensley, S. Chiao and C.-Y. Huang, 2002: Orographic Influences on Rainfall and Track Deflection Associated with the Passage of a Tropical Cyclone. *Mon. Wea. Rev.*, **130**, 2929–2950.

Liou, Y.-C., T.-C. Chen Wang, W.-C. Lee and Y.-J. Chang. 2006: The retrieval of asymmetric tropical cyclone structures using Doppler radar simulations and observations with the Extended GBVTD Technique. *Mon. Wea. Rev.*, **134**, 1140–1160.

Lonfat, M; Marks, FD; Chen, SS, 2004: Precipitation Distribution in Tropical Cyclones Using the Tropical Rainfall Measuring Mission (TRMM) Microwave Imager: A Global Perspective. *Mon. Weather Rev.*, **132**, 1645-1660.

Lorsolo, S., and J. L. Schroeder, 2006: Tower And Doppler Radar Observations From The Boundary Layer Of Hurricanes Isabel (2003) And Frances (2004). *Extended Abstracts, 27th Conference on Hurricanes and Tropical Meteorology*, Amer. Meteor. Soc., Monterey, Ca, 24 - 28 April. CD-ROM.

Mallen, K.J.m M.T. Montgomery and B. Wang, 2005: Reexamining the near-core radial structure of the tropical cyclone primary circulation: Implications for vortex resiliency. *J. Atmos. Sci.*, **62**, 408-425.

Mallett, W.A., 2000: *The Dynamics of the Atmospheric Boundary Layer of a Mature Tropical Cyclone: A Numerical Investigation*. PhD Thesis, James Cook University, Australia, 266 pp.

- Marks, F.D., and P. G. Black, 1990: Close encounter with an intense mesoscale vortex within Hurricane Hugo (September 15, 1989). *Extended Abstracts, Fourth Conf. on Mesoscale Processes*, Boulder, CO, Amer. Meteor. Soc., 114–115.
- Marks, F.D. P. Dodge and C. Sandin, 1999: WSR-88D Observations of hurricane atmospheric boundary layer structure at landfall. *Extended abstracts, 23rd Conference on Hurricanes and Tropical Meteorology*, Amer. Meteorol. Soc., Dallas, TX, Jan. 10-15. 1051-1055.
- May, P.T. 1996: The organization of convection in the rainbands of Tropical Cyclone Laurence. *Mon. Wea. Rev.*, **124**, 807-815.
- May, P.T. and G.J. Holland, 1999: The role of potential vorticity generation in tropical cyclone rainbands. *J. Atmos. Sci.*, **56**, 1224-1228.
- McNoldy, B. D., 2004, Triple eyewall in hurricane Juliette, *Bull. Amer. Meteor. Soc.*, **85**, 1663-1666.
- Möller, J.D. and M.T. Montgomery. 1999: Vortex Rossby Waves and Hurricane Intensification in a Barotropic Model. *J. Atmos. Sci.*, **56**, 1674–1687.
- Moeller, J. D., and M. T. Montgomery, 2000: Tropical cyclone evolution via potential vorticity anomalies in a three- dimensional balance model. *J. Atmos. Sci.*, **57**, 3366-3387.
- Möller, J. D., and L. J. Shapiro, 2002: Balanced contributions to the intensification on hurricane Opal as diagnosed from a GFDL model forecast. *Mon. Wea. Rev.*, **130**, 1866-1881.
- Möller, J.D. and L. J. Shapiro. 2005: Influences of Asymmetric Heating on Hurricane Evolution in the MM5. *J. Atmos. Sci.*: **62**, 3974–3992.
- Montgomery, M. T., and R. J. Kallenbach, 1997: A theory of vortex Rossby waves and its application to spiral bands and intensity changes in hurricanes. *Quart. J. Roy. Meteor. Soc.*, **123**, 435–465.
- Montgomery, M. T., H. D. Snell, and Z. Yang, 2001: Axisymmetric Spindown Dynamics of Hurricane-like Vortices. *J. Atmos. Sci.*, **58**, 421-435.
- Montgomery, M. T., V. A. Vladimirov, and P. V. Denissenko, 2002: An experimental study on hurricane mesovortices. *J. Fluid Mech.*, **471**, 1–32.
- Morrison, Ian, Steven Businger, Frank Marks, Peter Dodge and Joost A. Businger. 2005: An Observational Case for the Prevalence of Roll Vortices in the Hurricane Boundary Layer. *J. Atmos. Sci.*: **62**, 2662–2673.
- Moss, M.S. and S.L. Rosenthal, 1975: On the estimation of planetary boundary layer variables in mature hurricanes. *Mon. Wea. Rev.*, **103**, 980-988.
- Muramatsu, T., 1986: The structure of polygonal eye of a typhoon. *J. Meteor. Soc. Japan*, **64**, 913–921.
- National Research Council, 2004: *Assessment of the Benefits of Extending the Tropical Rainfall Measuring Mission: A Perspective from the Research and Operations Communities, Interim Report*. The National Academies Press, Washington, D. C.
- National Research Council, 2006: *NOAA's role in space-based global precipitation estimation and application*. The National Academies Press, Washington, D.C.

- Nolan, D.S. and B.F. Farrell, 1999a: Generalized Stability Analyses of Asymmetric Disturbances in One- and Two-Celled Vortices Maintained by Radial Inflow. *J. Atmos. Sci.*, **56**, 1282-1307.
- Nolan, D.S. and B.F. Farrell, 1999b: The intensification of two-dimensional swirling flows by stochastic asymmetric forcing. *J. Atmos. Sci.*, **56**, 3937-3962.
- Nolan, D.S., and Montgomery M.T., 2000: The algebraic growth of wavenumber one disturbances in hurricane-like vortices. *J. Atmos. Sci.* **57**, 3514-3538.
- Nolan, D.S., M.T. Montgomery, and L.D. Grasso, 2001: The Wavenumber-One Instability and Trochoidal Motion of Hurricane-like Vortices. *J. Atmos. Sci.*, **58**, 3243-3270.
- Nolan, D.S. and M.T. Montgomery, 2002: Nonhydrostatic, Three-Dimensional Perturbations to Balanced, Hurricane-like Vortices. Part I: Linearized Formulation, Stability, and Evolution. *J. Atmos. Sci.* **59**, 2989-3020.
- Nolan, D.S., and L. D. Grasso. 2003: Nonhydrostatic, Three-Dimensional Perturbations to Balanced, Hurricane-Like Vortices. Part II: Symmetric Response and Nonlinear Simulations. *J. Atmos. Sci.* **60**, 2717-2745.
- Nolan, D.S., 2005: Instabilities in hurricane-like boundary layers. *Dynamics of Atmospheres Oceans*: 40, 209-236
- Nolan, D.S., Y. Moon, and D. Stern, 2006: Tropical cyclone intensification from asymmetric convection: Energetics and efficiency. Submitted to *J. Atmos. Sci.*
- Nong, S. and K. Emanuel, 2003: A numerical study of the genesis of concentric eyewalls in hurricanes. *Quart. J. Roy. Meteor. Soc.*, 129, 3323-3338.
- Nuissier, Olivier; R. F. Rogers; F. Roux. 2005 : A numerical simulation of Hurricane Bret on 22-23 August 1999 initialized with airborne Doppler radar and dropsonde data. *Quart. J. Roy. Meteorol. Soc.* **131**, 155-194.
- Oda, Masahito, Toshihisa Itano, Gen'ichi Naito, Mikio Nakanishi and Kikuro Tomine. 2005: Destabilization of the Symmetric Vortex and Formation of the Elliptical Eye of Typhoon Herb. *J. Atmos. Sci.*: 62, 2965-2976.
- Ortt, D. and S.S. Chen, 2006: Rainbands and secondary eye wall formation as observed in RAINEX. *Extended Abstracts, 27th Conference on Hurricanes and Tropical Meteorology*, Amer. Meteor. Soc., Monterey, Ca, 24 - 28 April. CD-ROM.
- Paterson, Linda A., Barry N. Hanstrum, Noel E. Davidson and Harry C. Weber. 2005: Influence of Environmental Vertical Wind Shear on the Intensity of Hurricane-Strength Tropical Cyclones in the Australian Region. *Mon. Wea. Rev.*: 133, 3644-3660
- Peng, M.S., B.-F. Jeng and R. T. Williams. 1999: A Numerical Study on Tropical Cyclone Intensification. Part I: Beta Effect and Mean Flow Effect. *J. Atmos. Sci.*, **56**, 1404-1423.
- Persing, J., M.T. Montgomery and R.E. Tuleya, 2002: Environmental interactions in the GFDL hurricane model for Hurricane Opal. *Mon. Weea. Rev.*, **130**, 298 - 317.
- Persing, J. and M. T. Montgomery. 2003: Hurricane Superintensity. *J. Atmos. Sci.* **60**, 2349-2371.
- Persing, J. and Michael T. Montgomery. 2005: Is Environmental CAPE Important in the Determination of Maximum Possible Hurricane Intensity?. *J. Atmos. Sci.*: **62**, 542-550.

- Powell, M.D., 1980: Evaluations of diagnostic marine boundary-layer models applied to hurricanes. *Mon. Wea. Rev.*, **108**, 757-766.
- Powell, M.D., 1982: The transition of the Hurricane Frederic boundary-layer wind fields from the open Gulf of Mexico to landfall. *Mon. Wea. Rev.*, **110**, 1912-1932.
- Powell, M.D., 1987: Changes in the low-level kinematic and thermodynamic structure of Hurricane Alicia (1983) at landfall. *Mon. Wea. Rev.*, **115**, 75-99.
- Powell, M.D., 1990a: Boundary layer structure and dynamics in outer hurricane rainbands. Part I: Mesoscale rainfall and kinematic structure. *Mon. Wea. Rev.*, **118**, 891-917.
- Powell, M.D., 1990b: Boundary layer structure and dynamics in outer hurricane rainbands. Part II: Downdraft modification and mixed layer recovery. *Mon. Wea. Rev.*, **118**, 918-938.
- Powell, M.D. and P.G. Black, 1990: The relationship of hurricane reconnaissance flight-level wind measurements to winds measure by NOAA=s oceanic platforms. *J. Wind Engineering And Industrial Aerodynamics*, **36**, 381-392.
- Powell, M.D., P.D. Dodge and M.L. Black, 1991: The landfall of Hurricane Hugo in the Carolinas: Surface wind distribution. *Wea. and Forecasting*, **6**, 379-399.
- Powell, M.D., S.H. Houston and T.A. Reinhold, 1996: Hurricane Andrew=s landfall in south Florida. Part I: Standardizing measurements for documentation of surface wind fields. *Wea. and Forecasting*, **11**, 304-328.
- Powell, M.D. and S.H. Houston, 1996: Hurricane Andrew=s landfall in south Florida. Part II: Surface wind fields and potential real-time applications. *Wea. and Forecasting*, **11**, 329-349.
- Powell, M.D. and S.H. Houston, 1998: Surface wind fields of Hurricanes Erin, Opan, Luis, Marilyn and Roxanne at landfall. *Mon. Wea. Rev.*, **126**, 1259-1273.
- Powell, M.D., P.J. Vickery and T.A. Reinhold, 2003: Reduced drag coefficient for high wind speeds in tropical cyclones. *Nature*, **422**, 279-283.
- Reasor P. D., Montgomery M. T., Marks F. D. Jr., Gamache J. F., 2000: Low-wavenumber structure and evolution of the hurricane inner core observed by airborne dual-doppler radar. *Mon. Wea. Rev.* **128**, 1653-1680.
- Reasor, P.D., and M.T. Montgomery, 2001: Three-dimensional alignment and corotation of weak, TC-like vortices via linear vortex Rossby waves. *J. Atmos. Sci.*, **58**, 2306-2330.
- Reasor, P.D., M.T. Montgomery, and L.D. Grasso, 2004: A new look at the problem of tropical cyclones in vertical shear flow: Vortex resiliency. *J. Atmos. Sci.* **61**, 3-22.
- Reisner, J. M., A. Mousseau, A. A. Wyszogrodzki and D. A. Knoll. 2005: An Implicitly Balanced Hurricane Model with Physics-Based Preconditioning. *Mon. Wea. Rev.*: **133**, 1003–1022
- Romine, G.S. and R.B. Wilhelmson. 2006: Finescale spiral band features within a numerical simulation of Hurricane Opal (1995). *Mon. Wea. Rev.*, **134**, 1121–1139.
- Roux Frank, Chane-Ming F., Lasserre-Bigorry A. and Nuissier O.. 2004: Structure and Evolution of Intense Tropical Cyclone Dina near La Réunion on 22 January 2002: GB-EVTD Analysis of Single Doppler Radar Observations. *J. Atmos. Ocean. Tech.* **21**, 1501–1518.

- Rosenthal, S.L., 1962: *A theoretical analysis of the field of motion in the hurricane boundary layer*. National Hurricane Research Project Report No 56, Washington D.C., 12pp.
- Rozoff, C.M., W.H. Schubert, B.D. McNoldy and J.P. Kossin. 2006: Rapid filamentation zones in intense tropical cyclones. *J. Atmos. Sci.*, **63**, 325–340.
- Schechter, D.A., M.T. Montgomery, and P.D. Reasor, 2002: A theory for the vertical alignment of a quasigeostrophic vortex. *J. Atmos. Sci.*, **59**, 150-168.
- Schneider R. and G.M. Barnes, 2005: Low-Level Kinematic, Thermodynamic, and Reflectivity Fields Associated with Hurricane Bonnie (1998) at Landfall. *Mon. Wea. Rev.*, **133**, 3243-3259.
- Schroeder, J.L. and D.A. Smith, 2003: Hurricane Bonnie wind flow characteristics as determined from WEMITE. *J. Wind Engineering and Industrial Aerodynamics*, **91**, 767B789.
- Schubert, W.H., M.T. Montgomery, R.K. Taft, T.A. Guinn, S.R. Fulton, J.P. Kossin and J.P. Edwards, 1999: Polygonal eyewalls, asymmetric eye contraction, and potential vorticity mixing in hurricanes. *J. Atmos. Sci.*, **56**, 1197-1223.
- Schwendike, J., 2005: *The Boundary Layer Winds in Hurricanes Danielle (1998) and Isabel (2003)*. Diplomarbeit in Meteorology, Freie Universität, Berlin, 255pp.
- Shapiro, L.J., 1983: The asymmetric boundary layer under a translating hurricane. *J. Atmos. Sci.*, **40**, 1984-1998.
- Shapiro, L.J., and M.T. Montgomery, 1993: A three-dimensional balance theory for rapidly rotating vortices. *J. Atmos. Sci.*, **50**, 3322-3335.
- Shapiro, L.J., 2000: Potential vorticity asymmetries and tropical cyclone evolution in a three-layer model. *J. Atmos. Sci.*, **57**, 3645-3662.
- Shapiro, L.J. and J.D. Möller, 2003: Influence of Atmospheric Asymmetries on the Intensification of Hurricane Opal: Piecewise PV Inversion Diagnosis of a GFDL Model Forecast. *Mon. Wea. Rev.*, **131**, 1637-1649.
- Shapiro, L.J. and J.D. Möller, 2005: Influence of Atmospheric Asymmetries on the Intensification of GFDL Model Forecast Hurricanes. *Mon. Wea. Rev.*: **133**, 2860–2875
- Shen, W., I. Ginis, and R.E. Tuleya, 2002: An investigation of land surface water on landfalling hurricanes. *J. Atmos. Sci.*, **59**, 789-802.
- Simpson, R., 2003, *Hurricane!: Coping with disaster*, American Geophysical Union, Washington, D.C., 360 pp. Chapters by Gray, Rappaport and Simpson, Sheets, DeMaria and Gross, Frank, Myers and White, Pielke, Emanuel, Willoughby, Velden et al., Ritchie et al., Tyrell and Holland, Emmitt, Holland.
- Smith, R. K., W. Ulrich, and G. Sneddon, 2000: The dynamics of hurricane-like vortices in vertical shear flows. *Quart. J. Roy. Meteor. Soc.*, **126**, 2653-2670.
- Smith, R.K., 2003: A simple model of the hurricane boundary layer. *Quart. J. Royal Meteorol. Soc.*, **128**, 1007-1027. doi: 10.1256/qj.01.197
- Smith, R. K., 2005: "Why must hurricanes have eyes?" Revisited. *Weather*: **131**, 326-328
- Smith, R.K., M. T. Montgomery, and H. Zhu, 2005: Buoyancy in tropical cyclone and other rapidly

- rotating atmospheric vortices. *Dynamics of Atmospheres and Oceans*: **40**, 189-208.
- Smith, R.K, 2006: Accurate determination of a balanced axisymmetric vortex in a compressible atmosphere. *Tellus*. **58A**, 98-103.
- Spencer, R.W., H.M. Goodman, R.E. Hood, 1989: Precipitation retrieval over land and ocean with SSM/I: Identification and characteristics of the scattering signal. *J. Atmos. Ocean. Technol.*, **6**, 254-273.
- Stern, D.P. and S.D. Aberson, 2006: Extreme vertical winds measured by dropwindsondes in hurricanes. *Extended Abstracts, 27th Conference on Hurricanes and Tropical Meteorology*, Amer. Meteor. Soc., Monterey, Ca, 24 - 28 April. CD-ROM.
- Tonkin, H., Holland, G.J., Holbrook, N. and Henderson-Sellers, A. 2000: An evaluation of thermodynamic estimates of climatological maximum potential tropical cyclone intensity. *Mon. Wea. Rev.*, **128**, 746-762.
- Tuleya, R.E., M.A. Bender, and Y. Kurihara, 1984: Simulation study of the landfall of tropical cyclones, using a movable nested-mesh model. *Mon. Wea. Rev.*, **112**, 124-136.
- Tuleya, R.E., 1994: Tropical storm development and decay: sensitivity to surface boundary conditions. *Mon. Wea. Rev.*, **122**, 291-304.
- Velden, C. S. and J. D. Hawkins, 2002, The increasing role of weather satellites in tropical cyclone analysis and forecasting, *5th International Workshop on Tropical Cyclones (IWTC-V)*, Cairns, Australia, Dec.
- Velden, C., B. harper, F. Wells, J.L. Beven II, R. Zehr, T. Olader, M. Mayfield, C. Guard, M. Lander, R. Edson, L. Avila, A. Burton, M. Turk, A. Ikuchi, A. Christian, P. Caroffe and P. McCrone, 2006: The Dvorak tropical cyclone intensity estimation technique: A satellite-based method that has endured for over 30 years. *Bull Amer. Meteorol. Soc.*, in press.
- Wakimoto, R.M., and P.G. Black, 1994: Damage survey of Hurricane Andrew and its relationship to the eyewall. *Bull. Amer. Meteor. Soc.*, **75**, 189-200.
- Walsh, K.J.E. 2002: Probability of cyclone strike on specific regions of the Queensland coast, given current cyclone position and movement. *Australian Meteorological Magazine*. 51, 69-75.
- Wang, Y., and G.J. Holland, 1995: On the interaction of tropical-cyclone-scale vortices. IV: Baroclinic vortices. *Quart. J. Roy. Meteor. Soc.*, **121**, 95-126.
- Wang, Y., and G.J. Holland, 1996a: Beta drift of baroclinic vortices. Part I: Adiabatic vortices. *J. Atmos. Sci.*, **53**, 411-427.
- Wang, Y., and G.J. Holland, 1996b: Beta drift of baroclinic vortices. Part II: Diabatic vortices. *J. Atmos. Sci.*, **53**, 3737-3756.
- Wang, Y., and G.J. Holland, 1996c: Tropical cyclone motion and evolution in vertical shear. *J. Atmos. Sci.*, **53**, 3313-3332.
- Wang, Y., 2001: An Explicit Simulation of Tropical Cyclones with a Triply Nested Movable Mesh Primitive Equation Model: TCM3. Part I: Model Description and Control Experiment. *Mon. Wea. Rev.*, **129**, 1370-1394.

- Wang, Yuqing, 2002a: Vortex Rossby Waves in a Numerically Simulated Tropical Cyclone. Part I: Overall Structure, Potential Vorticity, and Kinetic Energy Budgets. *J. Atmos. Sci.*, **59**, 1213-1238.
- Wang, Yuqing, 2002b: Vortex Rossby Waves in a Numerically Simulated Tropical Cyclone. Part II: The Role in Tropical Cyclone Structure and Intensity Changes. *J. Atmos. Sci.*, **59**, 1239-1262.
- Wang, Y., 2002c: An explicit simulation of tropical cyclones with a triply nested movable mesh primitive equation model: TCM3. Part II: Some model refinements and sensitivity to cloud microphysics parameterization. *Mon. Wea. Rev.*, **130**, 3022–3036
- Wang, Y., M.T. Montgomery, and B. Wang, 2004: How much vertical shear can a well-developed tropical cyclone resist? *Preprints of the 26th Conference on Hurricanes and Tropical Meteorology*, 3-7 May 2004, Miami, Florida, 100-101.
- Wang, Y. and C.-C. Wu. 2004: Current understanding of tropical cyclone structure and intensity changes - a review. *Meteorol. and Atmos. Phys.*: **87**, 257 - 278.
- Wessel, J., J. Cornelius, R. W. Farley, A. Fote, J. Haferman, B. Gardiner, Y. Hong, D. B. Kunkee, G. Poe, S. D. Swadley, D. J. Tesmer, B. H. Thomas, E. Uliana, and D. Boucher, 2004: First observations from the DMSP SSMIS, 13th AMS Conference on Satellite Meteorology and Oceanography.
- Willoughby, H.E., 1978: A possible mechanism for the formation of hurricane rainbands. *J. Atmos. Sci.*, **35**, 838-848.
- Willoughby, H.E., J.A. Clos and M.G. Shoreibah. 1982: Concentric Eye Walls, Secondary Wind Maxima, and The Evolution of the Hurricane vortex. *J. Atmos. Sci.*, **39**, 395–411.
- Willoughby, H.E., F.D. Marks Jr. and R.J. Feinberg. 1984: Stationary and Moving Convective Bands in Hurricanes. *J. Atmos. Sci.*, **41**, 3189–3211.
- Willoughby, H.E. and M.E. Rahn, 2004: Parametric representation of the primary hurricane vortex. Part I: Observations and evaluation of the Holland (1980) model. *Mon. Wea. Rev.*, **132**, 3033 - 3048.
- Willoughby, H.E., R.W.R. Darling and M.E. Rahn, 2006: Parametric representation of the primary hurricane vortex. Part II: A new family of sectionally continuous profiles. *Mon. Wea. Rev.*, **134**, 1102-1120.
- Wong, M. L. M. and J. C. L. Chan, 2004: Tropical cyclone intensity in vertical wind shear. *J. Atmos. Sci.*: **61**, 1859-1876.
- Wroe, D.R. and G.M. Barnes. 2003: Inflow Layer Energetics of Hurricane Bonnie (1998) near Landfall. *Mon. Wea. Rev.*, **131**, 1600–1612.
- Wu, C.-C. and K.A. Emanuel. 1993: Interaction of a Baroclinic Vortex with Background Shear: Application to Hurricane Movement. *J. Atmos. Sci.*, **50**, 62–76.
- Wu C.-C., 2001: Numerical simulation of Typhoon Gladys (1994) and its interaction with Taiwan terrain using GFDL hurricane model. *Mon. Wea. Rev.*, **129**, 1533–1549.
- Wu C.-C., Emanuel K.A., 1993: Interaction of a baroclinic vortex with background shear: Application to hurricane movement. *J. Atmos. Sci.*, **50**, 62–76.
- Wu C.-C., Cheng H.-J., 1999: An observational study of environmental influences on the intensity changes of typhoons Flo (1990) and Gene (1990). *Mon. Wea. Rev.*, **127**, 3003–3031.

- Wu C.-C., Kuo Y.-H., 1999: Typhoons affecting Taiwan: Current understanding and future challenges. *Bull. Amer. Meteor. Soc.*, **80**, 67–80.
- Wu C.-C., Yen T.-H., Kuo Y.-H., Wang Y., 2002: Rainfall simulation associated with typhoon Herb (1996) near Taiwan. Part I: The topographic effect. *Wea. Forecast.*, **17**, 1001–1015.
- Wu C.-C., Chou K.-H., Cheng H.-J., Wang Y., 2003: Eyewall contraction, breakdown and reformation in a landfalling typhoon. *Geophys. Res. Lett.*, **30**, 1887; DOI: 10.1029=2003GL017653.
- Wu, Liguang and S.A. Braun. 2004: Effects of Environmentally Induced Asymmetries on Hurricane Intensity: A Numerical Study. *J. Atmos. Sci.*: 61, 3065-3081.
- Wurman, J. and J. Winslow, 1998: Intense sub-kilometre-scale boundary layer rolls observed in Hurricane Fran. *Science*, **280**, 555-557.
- Yau, M. K., Y. Liu, D.-L. Zhang and Y. Chen. 2004: A Multiscale Numerical Study of Hurricane Andrew (1992). Part VI: Small-Scale Inner-Core Structures and Wind Streaks. *Mon. Wea. Rev.*: 132, 1410-1433.
- Yeh, T.-C. and R.L. Elsberry. 1993: Interaction of Typhoons with the Taiwan Orography. Part I: Upstream Track Deflections. *Mon. Wea. Rev.*, **121**, 3193–3212.
- Yeh, T.-C. and R.L. Elsberry. 1993: Interaction of Typhoons with the Taiwan Orography. Part II: Continuous and Discontinuous Tracks across the Island. *Mon. Wea. Rev.*, **121**, 3213–3233.
- Zeng, Z., Y. Wang, and C.-C. Wu, 2006: Environmental dynamical control of tropical cyclone intensity - An observational study. *Mon. Wea. Rev.*, in press.
- Zhang, D.-L., Y. Liu and M. K. Yau. 2000: A Multiscale Numerical Study of Hurricane Andrew (1992). Part III: Dynamically Induced Vertical Motion. *Monthly Weather Review*: **128**, 3772–3788
- Zhang, D.-L., Y. Liu, and M. K. Yau, 2001: A Multiscale Numerical Study of Hurricane Andrew (1992). Part IV: Unbalanced Flows. *Mon. Wea. Rev.*, **129**, 92-107.
- Zhang, D. L., Y. Liu, and M. K. Yau, 2002: A multiscale numerical study of hurricane Andrew(1992). Part V: Inner core thermodynamics. *Mon. Wea. Rev.*, **130**, 2745-2763.
- Zhang, Da-Lin; Kieu, Chanh Q. 2005: Shear-Forced Vertical Circulations in Tropical Cyclones. *Geophys. Res. Lett.*: **32**, L13822.
- Zhang, Q.-H., S.-J. Chen, Y.-H. Kuo, K.-H. Lau and R.A. Anthes. 2005: Numerical Study of a Typhoon with a Large Eye: Model Simulation and Verification. *Mon. Wea. Rev.*: **133**, 725–742
- Zhu, Hongyan, Smith, Roger K., 2002: The Importance of Three Physical Processes in a Minimal Three-Dimensional Tropical Cyclone Model. *J. Atmos. Sci.*. 59, 1825-1840.
- Zhu, Hongyan, W. Ulrich and R. K. Smith. 2004: Ocean Effects on Tropical Cyclone Intensification and Inner-Core Asymmetries. *J. Atmos. Sci.*: 61, 1245-1258.